On the gigantic southeast Alaska landslide-generated tsunami of 10 August 2025 and its failure to reach the north coast of British Columbia

Alexander B. Rabinovich, Richard E. Thomson, Denny C. Sinnott,
David A. Riedel, Fred E. Stephenson

Fisheries and Oceans Canada
Institute of Ocean Sciences
9860 West Saanich Road
Sidney, BC
V8L 4B2

2026

Canadian Technical Report of
Hydrography and Ocean Sciences 430

Fisheries and Oceans Canada | Pêches et Océans Canada

Canada

Canadian Technical Report of Hydrography and Ocean Sciences

Technical reports contain scientific and technical information of a type that represents a contribution to existing knowledge but which is not normally found in the primary literature. The subject matter is generally related to programs and interests of the Oceans and Science sectors of Fisheries and Oceans Canada.

Technical reports may be cited as full publications. The correct citation appears above the abstract of each report. Each report is abstracted in the data base *Aquatic Sciences and Fisheries Abstracts.*

Technical reports are produced regionally but are numbered nationally. Requests for individual reports will be filled by the issuing establishment listed on the front cover and title page.

Regional and headquarters establishments of Ocean Science and Surveys ceased publication of their various report series as of December 1981. A complete listing of these publications and the last number issued under each title are published in the *Canadian Journal of Fisheries and Aquatic Sciences*, Volume 38: Index to Publications 1981. The current series began with Report Number 1 in January 1982.

Rapport technique canadien sur l'hydrographie et les sciences océaniques

Les rapports techniques contiennent des renseignements scientifiques et techniques qui constituent une contribution aux connaissances actuelles mais que l'on ne trouve pas normalement dans les revues scientifiques. Le sujet est généralement rattaché aux programmes et intérêts des secteurs des Océans et des Sciences de Pêches et Océans Canada.

Les rapports techniques peuvent être cités comme des publications à part entière. Le titre exact figure au-dessus du résumé de chaque rapport. Les rapports techniques sont résumés dans la base de données *Résumés des sciences aquatiques et halieutiques*.

Les rapports techniques sont produits à l'échelon régional, mais numérotés à l'échelon national. Les demandes de rapports seront satisfaites par l'établissement auteur dont le nom figure sur la couverture et la page de titre.

Les établissements de l’ancien secteur des Sciences et Levés océaniques dans les régions et à l'administration centrale ont cessé de publier leurs diverses séries de rapports en décembre 1981. Vous trouverez dans l'index des publications du volume 38 du *Journal canadien des sciences halieutiques et aquatiques*, la liste de ces publications ainsi que le dernier numéro paru dans chaque catégorie. La nouvelle série a commencé avec la publication du rapport numéro 1 en janvier 1982.

.

Canadian Technical Report of
Hydrography and Ocean Sciences 430

2026

On the gigantic southeast Alaska landslide-generated tsunami of 10 August 2025 and its failure to reach the north coast of British Columbia

by

Alexander B. Rabinovich, Richard E. Thomson, Denny C. Sinnott, David A. Riedel, Fred E. Stephenson

Fisheries and Oceans Canada
Institute of Ocean Sciences
9860 West Saanich Road
Sidney, BC
V8L 4B2

© His Majesty the King in Right of Canada, as represented by the Minister of the Department of Fisheries and Oceans, 2026

This work is licensed under the Open Government Licence

Cat. No. Fs 97-18/430E-PDF ISBN 978-1-100-01371-8 ISSN 1488-5417

https://doi.org/10.60825/agsp-ja69

Correct citation for this publication:

Rabinovich, A.B., Thomson, R.E., Sinnott, D.C., Riedel, D.A., Stephenson, F.E. 2026. On the gigantic southeast Alaska landslide-generated tsunami of 10 August 2025 and its failure to reach the north coast of British Columbia. Can. Tech. Rep. Hydrogr. Ocean Sci. 430: v + 36 p. https://doi.org/10.60825/agsp-ja69

TABLE OF CONTENTS

1. INTRODUCTION……..1

2. LANDSLIDE-GENERATED TSUNAMIS ALONG THE PACIFIC COAST OF NORTH AMERICA…….2

2.1. Historical Kwalate landslide and tsunami…….6

2.2. The 1958 Lituya Bay tsunami…….9

2.3. The 2015 Taan Fjord tsunami……..11

3. TRACY ARM LANDSLIDE AND TSUNAMI…….....14

3A. TIDE GAUGE OBSERVATIONS……..……..……21

3B. RESULTS……..……..……23

4. SUMMARY AND CONCLUSIONS…….…….29

5. SUPPLEMENT: *Science* publication on the Tracy Arm landslide and tsunami……30

ACKNOWLEDGEMENTS…..…….……..32

REFERENCES……..……33

ABSTRACT

Rabinovich, A.B., Thomson, R.E., Sinnott, D.C., Riedel, D.A., Stephenson, F.E. 2026. On the gigantic southeast Alaska landslide-generated tsunami of 10 August 2025 and its failure to reach the north coast of British Columbia. Can. Tech. Rep. Hydrogr. Ocean Sci. 430: v + 36 p. https://doi.org/10.60825/agsp-ja69

A huge rockfall in Tracy Arm in Southeast Alaska at 13:26 UTC on 10 August 2025 generated a gigantic tsunami with an estimated local runup of 470-500 m – the second largest height ever recorded after the 1958 Lituya Bay tsunami runup of 525 m (also in Southeast Alaska). This report presents an analysis of the Tracy Arm tsunami along with a review of several major landslides and associated tsunamis that occurred on the coasts of British Columbia and southeastern Alaska. Major focus is on three of the most destructive events: (1) the Kwalate historical event (~1570 AD); (2) the 1958 Lituya Bay event; and (3) the 2015 Taan Fjord event. The scale, physical mechanisms and properties of these three landslides and tsunamis are very similar to those generated by the 2025 Tracy Arm failure.

For this study, we examined all available information on the 2025 Tracy Arm event, including photos, videos and satellite imagery. We also examined data from six NOAA tide gauges located in the vicinity of the slide and from six Canadian Hydrographic Survey tide gauges located in northern British Columbia. A tsunami wave was evident in only one station, Juneau, the closest to the landslide source area. The first tsunami wave arrived at Juneau at 14:12 UTC, i.e., 46 min after the landslide. The maximum recorded tsunami amplitude at Juneau was 27.6 cm, and the maximum trough-to-crest range 56.3 cm. The recorded tsunami amplitudes at this station were attenuated because the sampling interval (6 min) was too long; actual tsunami waves were likely about 1.5 times higher. No tsunami signal was detected at the 11 other stations, including the 6 stations located in northern British Columbia, demonstrating that landslide-generated tsunamis, even so massive as the 2025 Tracy Arm tsunami, typically have a local character and do not propagate far from the source area. An important lesson from the 2025 Tracy Arm event is the necessity for thorough examination and modelling of possible submarine sliding/slumping and slide-generated tsunamis in areas of existing and new construction, especially in the vicinity of unstable sediment accumulation.

RÉSUMÉ

Rabinovich, A.B., Thomson, R.E., Sinnott, D.C., Riedel, D.A., Stephenson, F.E. 2026. On the gigantic southeast Alaska landslide-generated tsunami of 10 August 2025 and its failure to reach the north coast of British Columbia. Can. Tech. Rep. Hydrogr. Ocean Sci. 430: v + 36 p. https://doi.org/10.60825/agsp-ja69

Un éboulement massif survenu à Tracy Arm, dans le sud-est de l'Alaska, le 10 août 2025 à 13 h 26 UTC, a engendré un tsunami gigantesque dont la hauteur de remontée locale (*runup*) est estimée entre 470 et 500 m ; il s'agit de la deuxième hauteur la plus importante jamais enregistrée, après celle de 525 m observée lors du tsunami de la baie Lituya en 1958 (également dans le sud-est de l'Alaska). Ce rapport présente une analyse du tsunami de Tracy Arm ainsi qu'un examen de plusieurs glissements de terrain majeurs et des tsunamis associés survenus sur les côtes de la Colombie-Britannique et du sud-est de l'Alaska. L'étude se concentre principalement sur trois des événements les plus destructeurs : (1) l'événement historique de Kwalate (vers 1570 apr. J.-C.) ; (2) l'événement de la baie Lituya en 1958 ; et (3) l'événement du fjord Taan en 2015. L'ampleur, les mécanismes physiques et les caractéristiques de ces trois glissements de terrain et tsunamis sont très similaires à ceux engendrés par l'effondrement de Tracy Arm en 2025.

Pour cette étude, nous avons examiné toutes les informations disponibles concernant l'événement de Tracy Arm de 2025, notamment les photos, les vidéos et les images satellites. Nous avons également analysé les données provenant de six marégraphes de la NOAA situés à proximité du glissement de terrain et de six marégraphes du Service hydrographique du Canada situés dans le nord de la Colombie-Britannique. Une onde de tsunami n'a été clairement observée qu'à une seule station, celle de Juneau, la plus proche de la zone source du glissement. La première onde de tsunami a atteint Juneau à 14 h 12 UTC, soit 46 minutes après le glissement de terrain. L'amplitude maximale du tsunami enregistrée à Juneau était de 27,6 cm, et l'amplitude crête-creux maximale de 56,3 cm. Les amplitudes enregistrées à cette station étaient atténuées en raison d'un intervalle d'échantillonnage trop long (6 minutes) ; les ondes réelles du tsunami étaient probablement environ 1,5 fois plus élevées. Aucun signal de tsunami n'a été détecté aux 11 autres stations, y compris les 6 stations situées dans le nord de la Colombie-Britannique, ce qui démontre que les tsunamis générés par des glissements de terrain — même d'une ampleur telle que celui de Tracy Arm en 2025 — ont généralement un caractère local et ne se propagent pas loin de la zone source. L'événement de Tracy Arm de 2025 met en évidence la nécessité d'examiner et de modéliser minutieusement les risques potentiels de glissements ou d'effondrements sous-marins et les tsunamis qu'ils pourraient engendrer dans les zones de construction existantes ou nouvelles, en particulier à proximité d'accumulations de sédiments instables.



Oblique aerial photo of the 2025 Tracy Arm landslide captured during a field reconnaissance overflight on 13 August 2025. Look direction is to the west. (From USGS Public Domain)

1. INTRODUCTION

On 10 August 2025, a huge rockfall in Tracy Arm in Southeast Alaska generated a gigantic landslide tsunami with an estimated local runup of almost 500 m, comparable to the 1958 Lituya Bay tsunami runup, the highest ever observed. Although there were no tide gauges in the vicinity of Tracy Arm, a NOAA[1] instrument installed in Juneau, SE Alaska, recorded a significant train of tsunami waves. Based on the Juneau recording, we assumed that the Tracy Arm tsunami could affect not only the nearby coast of southeastern Alaska but also propagate southward to northern British Columbia. This was an extraordinary event that requires a detailed investigation.

The purpose of the present study is to examine all available tide gauge records and other information on Tracy Arm tsunami for the coast of British Columbia and adjacent region of Southeast Alaska. The resulting analysis enabled us to estimate statistical and spectral characteristics of the observed waves at various sites. This, in turn, makes it possible to deduce the physical mechanism of the recorded waves and potential risk of landslides and associated

[1] NOAA = National Oceanic and Atmospheric Administration, USA

tsunamis for the coast of British Columbia. For completeness, our study also provides an overview of the general situation with landslides and associated tsunamis along the Pacific coast of North America, with specific attention to the strongest known historical and recent landslide events that also produced gigantic tsunami waves: the Kwalate rock avalanche of ~1400, the 1958 Lituya Bay landslide and the 2015 Taan Fjord landslide. These events have strong similarity with that of 10 August 2025 in Tracy Arm and appear to be characteristic of the most dangerous events that can occur in the study region.

2. LANDSLIDE-GENERATED TSUNAMIS ALONG THE PACIFIC COAST OF NORTH AMERICA

Submarine landslides, slumps, rockfalls and avalanches can produce significant tsunamis in coastal areas of the world oceans. Although landslide-generated tsunamis are much more localized than seismically generated tsunamis, they can be highly destructive, especially in inlets, fjords or other semi-enclosed embayments. In particular, the 1958 Lituya Bay (Alaska) rockslide caused a 525-m tsunami that strongly impacted the inlet (see Section 2.2). The 1963 Vaiont Valley (northeast Italy) event, associated with a massive rock failure into a reservoir in this valley, created a huge tsunami wave that overtopped the dam, destroyed a neighboring town and killed approximately 3,000 people [*Murty*, 1977]. A large submarine slump, triggered by the 1998 M_w 7.0 earthquake offshore of the northern coast of Papua New Guinea, caused a catastrophic tsunami that hit the coast, killed about 2,500 people and injured thousands [*Synolakis et al.*, 2002; *Davies et al.*, 2003].

Although studies of landslide-generated tsunamis have a long history, the events themselves are relatively rare. The greatly enhanced interest in this problem over the past 20 years can be linked to two main causes: (1) significant earthquakes accompanied by local landslides and related catastrophic tsunamis in Indonesia (1992), Papua New Guinea (1998), and Turkey (1999); and (2) the well-documented dock failure and related tsunami in Skagway, Alaska (1995).

The Skagway event of 4 November 1994 associated with the Pacific and Arctic Railway and Navigation Company (PARN) dock collapse was not very strong (maximum runup was approximately 11 m), but it claimed the life of one worker and caused an estimated $21 million damage [*Lander,* 1996]. The resulting intensive scientific discussion [cf. *Kulikov et al.*, 1996; *Kowalik,* 1997; *Plafker and Greene*, 1998; *Rabinovich et al.,* 1999] contributed to significant progress in numerical modelling of landslide generated tsunamis (a detailed description of the event was given by *Thomson et al.* [2001]).

In general, the dimensions of the initial slide source determine the spatial and temporal scales of the generated waves, leading to differences between seismically generated tsunamis and landslide generated tsunamis. Typical periods of seismic tsunamis are from several minutes to a few hours, whereas typical periods of slide-generated tsunamis are from 10-20 s to a few minutes. The normal duration of earthquakes is 10-20 s, which is negligible compared with the time of wave travel through the source area. Thus, a seismic source can be regarded as instantaneous and does not involve the interaction between the bottom displacement and the excited tsunami waves. On the contrary, landslides last for several minutes and even tens of minutes, making the interaction between surface waves and the moving slide body important.

Landslides and associated tsunamis occur in many various places around the world. However, the coasts of British Columbia (BC) and Alaska (AK) are regions where landslides, rock falls, avalanches and similar events are most frequent, especially in the inlets and narrow straits of the mainland coast. Noteworthy events include those in Lituya Bay, Yakutat, Russell Fjord, Skagway Harbor, Kitimat Arm and Tacoma (Figure 1); occasionally they are accompanied by the largest runups (e.g., the 1958 Lituya Bay, 2015 Taan Fjord and 2025 Tracy Arm). Primarily, the high rate of occurrence is due to the elevated seismicity in these regions as well as to aspects of the coastal geography, and other contributing factors. Figure 1 shows the locations of the main known landslide events along the Pacific coast of North America that had documented tsunamis.

Landslides arise through the long-time accumulation of sediment fractions in individual parts of the coast and seafloor (folds, talwegs, canyons) as a result of alluvial sedimentation in river deltas and gradual erosion of the coast due to washing out of coastal materials (sandy, clayey, silty, oozy and sandy-silty formations) by wind, runoff and waves. The erosional disintegration of rocks, which results in their detachment and fall, as well as snow avalanches and collapses of great ice masses, can also lead to the formation of major tsunamis. In particular, glacier failures have repeatedly caused large tsunami waves in Yakutat Bay and Russell Fjord in southeastern Alaska (Figure 1). Significant sediment deposits are built up over time at the mouths of rivers. Most North American inlets have a river delta at their heads. These river deltas are adjacent to deep water and are therefore susceptible to slumping and tsunami generation. Studies in the coastal areas of Alaska, British Columbia, Washington, Oregon, and California indicate high instability of deltaic and nearshore sediments [cf. *Prior et al.*, 1981, 1984]. Large accumulations of unstable sediments deposited in the deltas of North American rivers, such as the Fraser, Skeena, and Nisqually, are particularly problematic [*Rabinovich et al.,* 2003].

Rabinovich et al. [2003] modelled the effects of potential subaerial slides on the Fraser River delta front in the Strait of Georgia and on the shores of Malaspina Strait. Results show that

sediment failure could generate tsunami wave heights of up to 18 m on the east coast of the Gulf Islands and up to 6-8 m along the east coast of Texada Island in the case of a Malaspina Strait event. Some rivers and lakes in BC are also at risk of landslide generated tsunamis; documented landslide events include the Fraser River at Haney (1880), the Thompson River at Spences Bridge (1905), Kitimat Arm (1975), Troitsa Lake (1998) and Chehalis Lake (2007) [*Evans*, 2001; *Brideau et al.,* 2012]. Other lakes with geographic tsunami potential are Harrison Lake in SW British Columbia and Kootenay Lake in the SE interior.

Underwater slopes in fjords and inlets commonly attain a delicate equilibrium with the long-term marine conditions and character of sediments. This stability can be disrupted, leading to failure, by local earthquakes. The 1958 Lituya Bay rockslide and tsunami, as well as a similar event in 1899, were triggered by strong earthquakes [cf. *Miller*, 1960; *Lander*, 1996]. Submarine landslides that accompanied the 1964 "Good Friday" Alaskan earthquake generated tsunami runups of several tens of meters in parts of the Alaskan coast (Figure 1) [*Lander*, 1996]. The British Columbia earthquake of 23 June 1946 (M_w 7.3) produced several local tsunamigenic landslides and slumps along the coast of Vancouver Island; the only death from the event was caused by a slump-generated tsunami overturning a small boat near Deep Bay [*Rogers*, 1980].

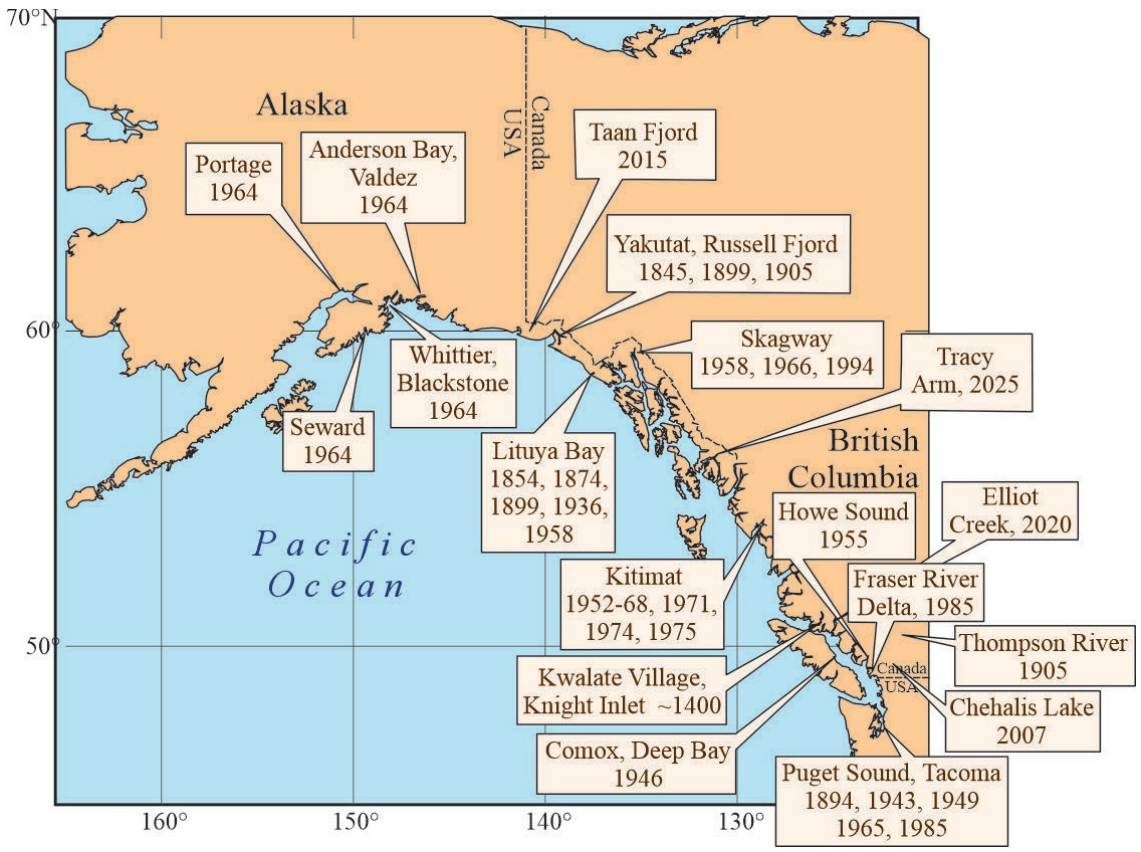


Figure 1. Locations of known submarine landslides and landslide-generated tsunamis along the west coast of North America.

Damaging submarine landslides can also be produced by local processes in the absence of seismic events [*Evans*, 2001]. In particular, the 1854, 1874, and 1936 Lituya Bay tsunamis and the 1974 and 1975 Kitimat slides and tsunamis occurred during seismically quiet periods. The 1975 Kitimat Arm failure and tsunami occurred at an extreme low tide (Figure 5.3a) that was coincident with coastal construction activity [*Prior et al*., 1984; *Kulikov et al.*, 1998]. The 1966 and 1994 Skagway Harbor events also coincided with anomalously low tides at a time of no seismic activity [*Lander*, 1996; *Kulikov et al.*, 1998; *Thomson et al.*, 2001). Sudden deposition of large sediment loads, especially in deltaic areas during flooding, erosion of the base of a slope, or construction-related loads and activity, as well as meteorological factors, such as heavy rainfall, strong winds, and atmospheric pressure change, are common triggers of subaerial slope failures in coastal zones [cf. *Evans*, 2001; *Rabinovich et al*., 2003].

In August 1905, a large landslide took place on the right bank of the Thompson River opposite the town of Spences Bridge in southwestern British Columbia. The landslide generated a displacement wave that ran up the opposite riverbank to a height of 22.5 m, destroyed many buildings in the settlement and killed 15 people [*Evans*, 2001]. Other locations in British Columbia where landslides have been reported include Howe Sound [*Terzaghi*, 1956] and the Fraser River delta region [*Hamilton and Wigen*, 1987] (Figure 1).

In British Columbia, well documented tsunamis caused by landslides were reported in Douglas Channel at Kitimat (1975), in Chehalis Lake (2007) and in Elliot Creek (2020) (Figure 1). These tsunamis were not associated with earthquakes but occurred when heavy rains caused changes in the groundwater conditions. The major submarine slope failure at the head of Kitimat Arm on 27 April 1975 resulted in the downslope movement of a large volume of sediments that produced substantial damage to nearby dock facilities and coastal settlements. Following this major slide, waves up to 8.2 m were generated. The tsunami oscillations lasted for about 1 hour and were responsible for the destruction of boats, docks and other property [*Murty,* 1979; *Skvortsov and Bornhold*, 2007].

The landslide and tsunami in Chehalis Lake (a small approximately 8 km long and 1 km wide lake located in the coastal mountains of British Columbia about 80 km east of Vancouver) is another example of a major tsunamigenic event. The landslide occurred along the northwestern shore of the lake on 4 December 2007 during a period of heavy rain. An intense water-on-snow meteorological event is thought to have triggered the slide [*Brideau et al.*, 2011]. The rock mass, with a volume of approximately 3 million m^3, travelled obliquely into a steep gully for approximately 900 m to the west shore of the lake and produced a tsunami with a maximum runup height of 37.8 m directly across the lake from the slide area [*Wang et al.*, 2015]. Measured

runup heights were 20 m or more throughout the northern portion of the lake, with heights of 4–10 m measured in the central and southern portions of the lake. A campground opposite the slide site was destroyed, and two other campgrounds on the lake were severely damaged by the tsunami. Fortunately, there was no one at the campground at the time.

An event similar to that in Chehalis Lake occurred on 28 November 2020 in the Elliot Creek area in the southern Coast Mountains of British Columbia. A small, unofficially named, glacial lake, Elliot Lake is located in a valley near the head of Bute Inlet, about 210 km northwest of Vancouver. About 18 million m^3 of rock slid down the steep west side of the valley across the toe of a glacier and travelled along a creek before entering the lake, producing a runup of more than 100 m [*Geertsema et al.*, 2022]. The lake is very remote, and it was not until two weeks after the event that the effects of this landslide were observed by forestry workers. The landslide's time of occurrence was determined from regional seismic network data. The field survey provided by *Geertsema et al.* [2022] indicated that the slide's volume was much larger than that of the 2007 Chehalis Lake event (~3 million m^3). The Elliot Lake landslide was a "significant" slide when compared against the largest observed slide in Canadian history, the Hope Slide in 1965, with an approximate volume of 47 million m^3. As shown by field survey data, the tsunami produced a trimline on both sides of the lake, with a maximum runup of 114 m on the west side of the lake and 73 m on the east side of the lake.

Climate change is driving worldwide glacial retreat. The removal of glacial ice supporting steep slopes, combined with the thawing of permafrost in alpine regions, increases the likelihood of landslides. These landslides, with the potential to generate tsunami runups far greater than most seismically generated tsunamis, are of extreme importance. Fortunately, both the 2007 Chehalis Lake and the 2020 Elliot Lake tsunami occurred in remote locations and resulted in no loss of life. They do, however, demonstrate the high risk of such events for the coasts of Alaska and British Columbia.

2.1. Historical Kwalate landslide and tsunami

The BC coastline consists of many long, deep (of 500 m or more) inlets bounded by steep sided mountains rising to heights of over 1700 m. These coastal features commonly have a limited population, but in summer they are visited by numerous boaters, kayakers and other recreational users. Rock and ice failures, snow avalanches and sediment slides are quite common in these inlets [*Bornhold and Thomson*, 2012]. One of the principal inlets of the British Columbia coast is Knight Inlet, which is about 125 km long and about 2.5 km wide (Figure 2). The inlet's opening is located just north of the upper part of Johnstone Strait, separating Vancouver Island from the mainland. Historical reports and field survey results indicate that in approximately 1570 AD a

highly catastrophic tsunami (the "*Kwalate tsunami*") occurred in this inlet, generated by a huge rock failure with a slide volume of approximately 3-4 million m^3 [*Bornhold et al.*, 2007].

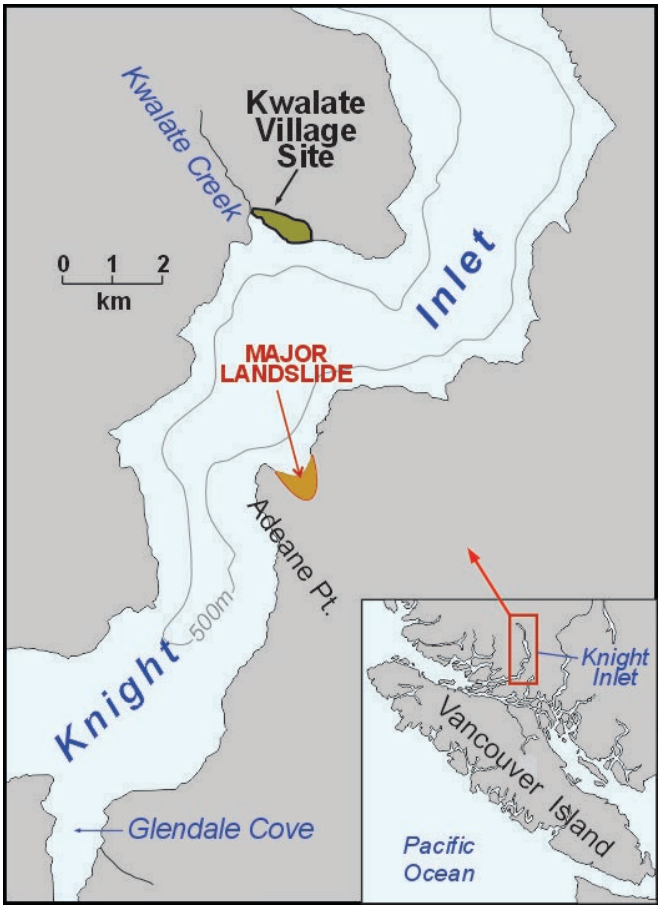


Figure 2. Map of Knight Inlet, the former First Nations village of Kwalate and the large landslide areas opposite the village site. Water depths are in metres. (Modified from [*Bornhold et al.*, 2007]).

The First Nations village of Kwalate was located at the mouth of the Kwalate River in the inlet (Figure 2). According to Kwakwaka'wakw oral narratives of the A'wa'etlala and Da'naxda'xw peoples, a devastating landslide-generated tsunami destroyed the village: "*About three generations ago, or possibly at an earlier date, a large portion of the mountain opposite Kwalate Point slid into the inlet causing a huge tidal wave which wiped out all of the inhabitants of the village opposite…and the vast slide is noticeable today*". "*Kwalate was the site of a big village at one time. The story I was told is that a big part of the mountain across the inlet fell into the sea and created a tidal wave that rolled across the inlet and drowned most of the village*" [*Bornhold et al.*, 2007].

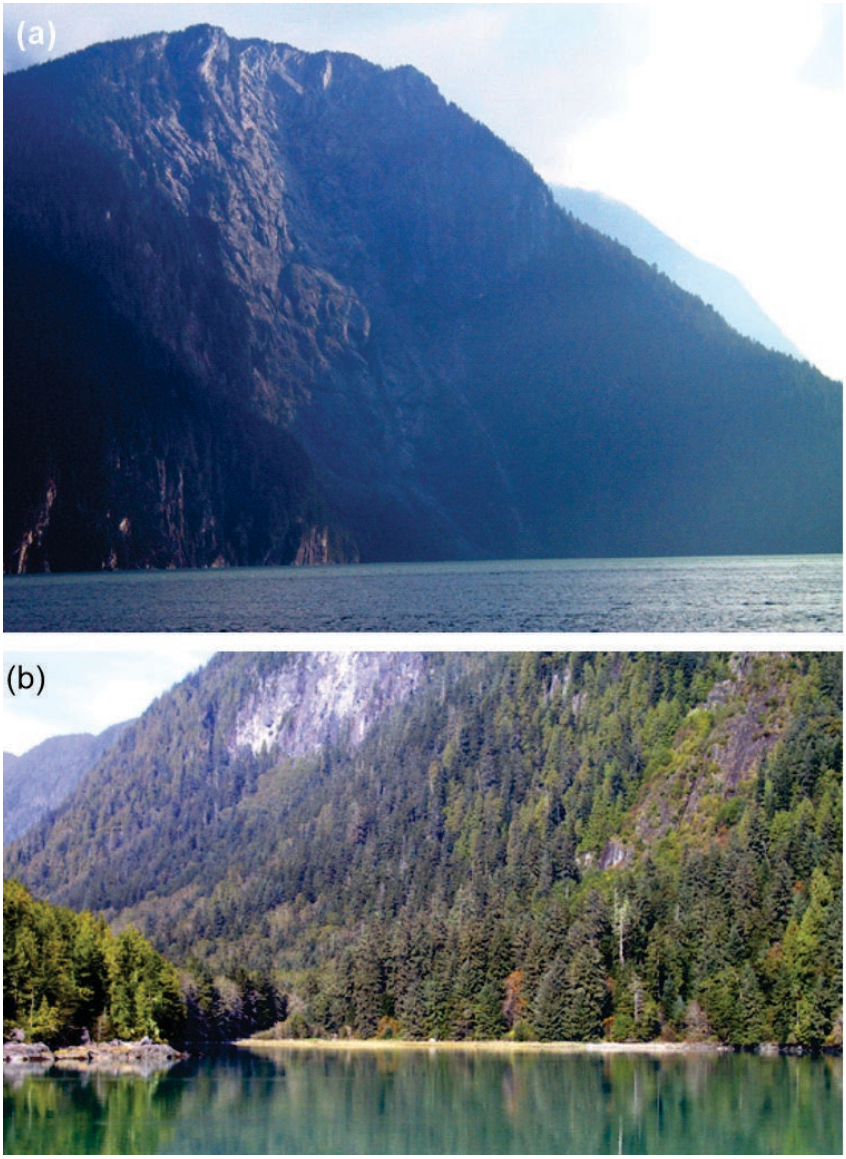


Figure 3. (a) Rock-avalanche area north of Adeane Point, Knight Inlet (right); the source of the Kwalate tsunami; (b) The mouth of the Kwalate River and the location of former Kwalate Village.

Bornhold et al. [2007] examined physical evidence of the Kwalate event, which included detailed shipboard bathymetric charting of the inlet, remotely operated vehicle surveys of the landslide debris on the seafloor and empirical modelling of the tsunami generation. Also, archaeological surveys were conducted to locate and test the remains of the village and there was an archival research of ethnographic and historical documents plus an interview with the First Nation hereditary chief, William Glendale II. The findings of these studies indicated that the Kwalate tsunami was generated by a rock avalanche originating from the 840-m high cliff face north-east of Adelaine Point (Figures 2 and 3a). On the opposite side of Knight Inlet, near the mouth of the Kwalate River, a 120-m long, 10-15 m wide platform rises from the beach (Figure

3b). It was on this platform that the former village of Kwalate was discovered. The debris found on the platform, together with hearth features and various fragments, show that the village, with an estimated total population of 100 or more, was totally swept away by the landslide-generated tsunami.

The landslide scar at Adeane Point is still visible across the inlet from the archaeological remains of Kwalate Village (Figure 3a). A prominent cone of coarse debris extending about 800 m from the shoreline was found at the bottom at the base of the landslide. The diameter of the cone at its terminus is about 400 m and the estimated volume of the debris is 4×10^6 m^3 [*Bornhold et al.*, 2007]. The estimated rock avalanche volume and morphology of the inlet between the slide and the village were used to determine the tsunami wave height that inundated the village. The estimates yield an initial wave height near the source as >25 m, while the wave height at the village was about 5-6 m.

As emphasized by *Bornhold et al.* [2007], the study documents that a devastating rock avalanche and associated tsunami likely destroyed the large aboriginal community of Kwalate Village located 5 km from the slide site and forever altered the history of First Nations peoples in the Knight Inlet area of British Columbia.

2.2. The 1958 Lituya Bay tsunami

The Lituya Bay tsunami of 10 July 1958 is the highest tsunami in recorded history, with the tsunami runup reaching a height of 525 m at the entrance of Gilbert Inlet (Figure 4) [*Lander*, 1996; *Fritz et al.*, 2009]. This megatsunami was caused by a major subaerial landslide triggered by a M_w 8.3 earthquake along the Fairweather Fault. The landslide area and the tsunami runup zone on the spur ridge directly on the opposite side of the inlet were clearly identified by post-event air photos, which show the landslide scar and the trimlines of the washed away forest [*Miller*. 1960].

Lituya Bay is a T-shaped tidal inlet of 14.5 km length and a maximum width of 3.2 km located in southeast Alaska (Figure 4). Two inlets at the head of the bay, Gilbert Inlet and Cerillion Inlet, form the upper bar ("roof") of Lituya Bay. The bay walls at the head are fjord-like glacially over-steeped. The landslide on the northeastern sidewall of Gilbert Inlet was triggered by the movement and intense seismic vibrations along the Fairweather Fault. The slide occurred in an area of active previous sliding and reached an elevation of 915 m along a steep slope. Using an approximately 40° angle slope angle [*Fritz et al.*, 2009], *Miller* [1960] estimated the slide volume as 30.6×10^6 m^3, which is of comparable magnitude to the estimated Hope Slide volume of 47×10^6 m^3 in 1965 noted previously.

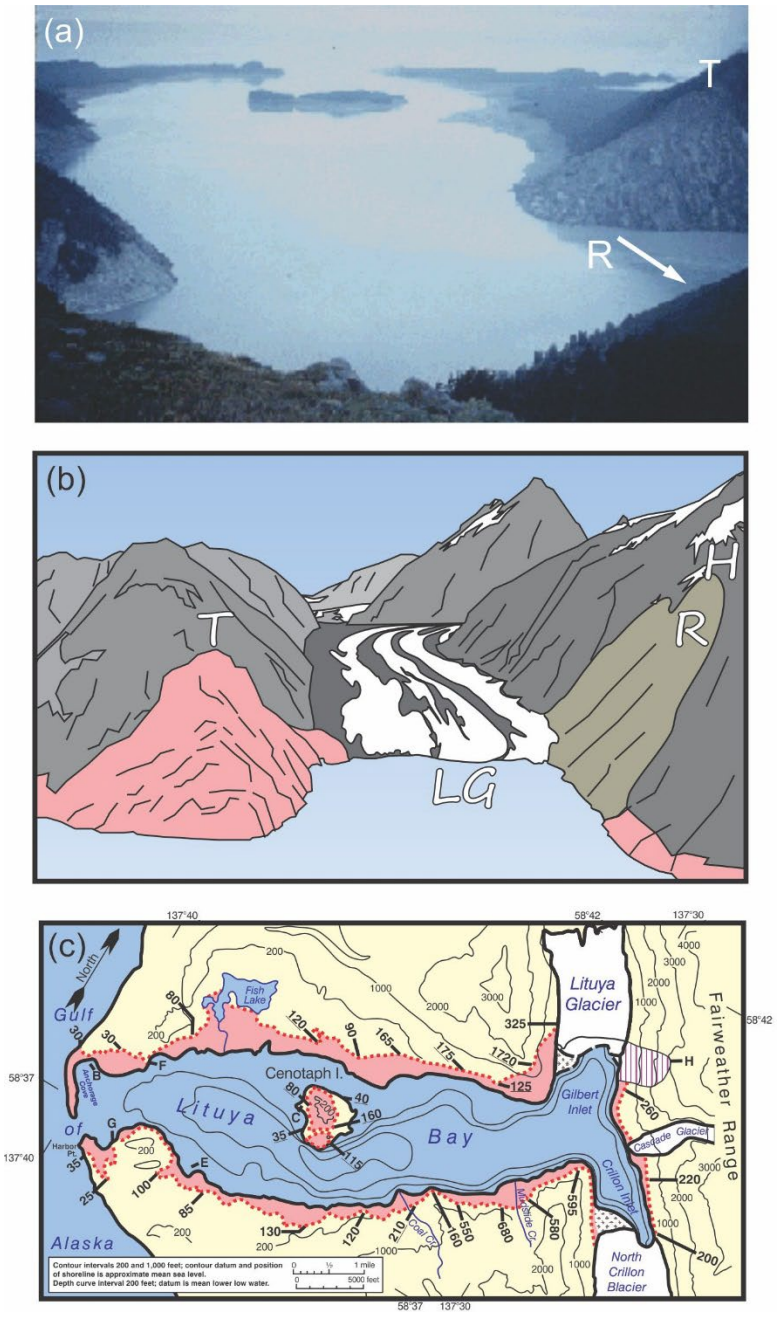


Figure 4. (a) Panoramic view of Lituya Bay from the head of the bay; "T" indicates the tsunami inundation zone with maximum runup height of 525 m. The rockslide area is not seen but its position is denoted by a white arrow labelled "R"; (b) a sketch of the northern and northeastern parts of Lituya Bay; the rockslide ("R") plunged into Gilbert Inlet from the cliff off the front of Lituya Glacier ("LG"), causing water to surge up to 525 m ("T"). The head of the rockslide scar ("H") was at about 900 m elevation; and (c) map of Lituya Bay with geographical information and effects of the 1958 tsunami. The dashed and solid lines in Gilbert Inlet are the approximate positions of the shoreline and glacier before (7 July 1958) and after (11 July 1958) the tsunami. The pink area bordered by a red dotted line is the inundated zone; land contours and runup heights are in feet. (The map was prepared by the U.S. Geological Survey after the 1958 tsunami).

The maximum runup height of 525 m (524 m by some other sources) was much higher than the Empire State Building (443 m) and Eiffel Tower (324 m). The entire bay was flooded with the runup line (still visible) up to 213 m. The 55-foot boat "Sunmore" anchored near the bay outlet was swept against the cliffs and the crew (Orville Wagner and his wife Mickey) were lost [*Lander,* 1996]. However, no damage from this tsunami was reported beyond Lituya Bay. At Hilo, Hawaii, a local tide gauge recorded a 10-cm wave that arrived 6.7 h after the earthquake, but it is not clear if this wave was associated with the Lituya Bay slide or with the earthquake itself.

Post-event field surveys in Lituya Bay revealed the unique geological and tectonic setting of the bay. It was found that giant tsunami waves occurred at least five times during the last 200 years: 1854 (height 120 m), 1874 (25 m), 1899 (60 m), 1936 (150 m) and 1958 (525 m) [*Miller*, 1960; *Fritz et al*., 2009]. Frequent occurrence of giant waves in this bay, as compared to similar bays in Alaska and British Columbia, is attributed to the combined effect of steep, recently glaciated slopes, highly fractured rocks and deep water in an active fault zone, heavy rainfall, and frequent freezing and thawing [*Miller*, 1960].

2.3. The 2015 Taan Fjord tsunami

On 17 October 2015, a massive landslide and tsunami occurred at the head of Taan Fjord in southeastern Alaska (60.18ºN, 141.30ºW), about 500 km ESE from Anchorage. The fjord is an arm of Icy Bay within the Wrangell-St.Elias National Park & Preserve. This event is one of the largest ever recorded. A possible reason for this slide, as well as some other recent massive slides, is climate change, which is driving worldwide glacial retreat and thinning along unstable hillslopes [*Higman et al.*, 2018].

The event was detected within hours through automated seismological techniques. The methodology also enabled investigators to estimate the mass and direction of the slide - all of which were later confirmed by remote sensing. Using a variety of Digital Elevation Modeling (DEM) and imagery sources, as well as direct field observations, the research team of *Higman et al.* [2018] was able to estimate the landslide parameters, map the deposit thickness and to model the generated tsunami. Additional studies of subaerial and submarine slide deposits were provided by *Haeussler et al.* [2018] and *Dufresne et al.* [2018]. These studies indicated that the slope failure at the terminus of the Tyndall Glacier (Figure 5) had a volume of 7.6×10^7 m^3 (about 4 times that of the 2020 Elliot Lake event), of which 5.1×10^7 m^3 moved directly into Taan Fjord [*Haeussler et al.*, 2018]. The resulting tsunami had a maximum runup height of 193 m [*Higman*

et al., 2018]. The data from NGD C/WDS indicates that the Taan Fjord tsunami had the fourth largest runup of this group, with Lituya Bay (1958) having the largest runup.

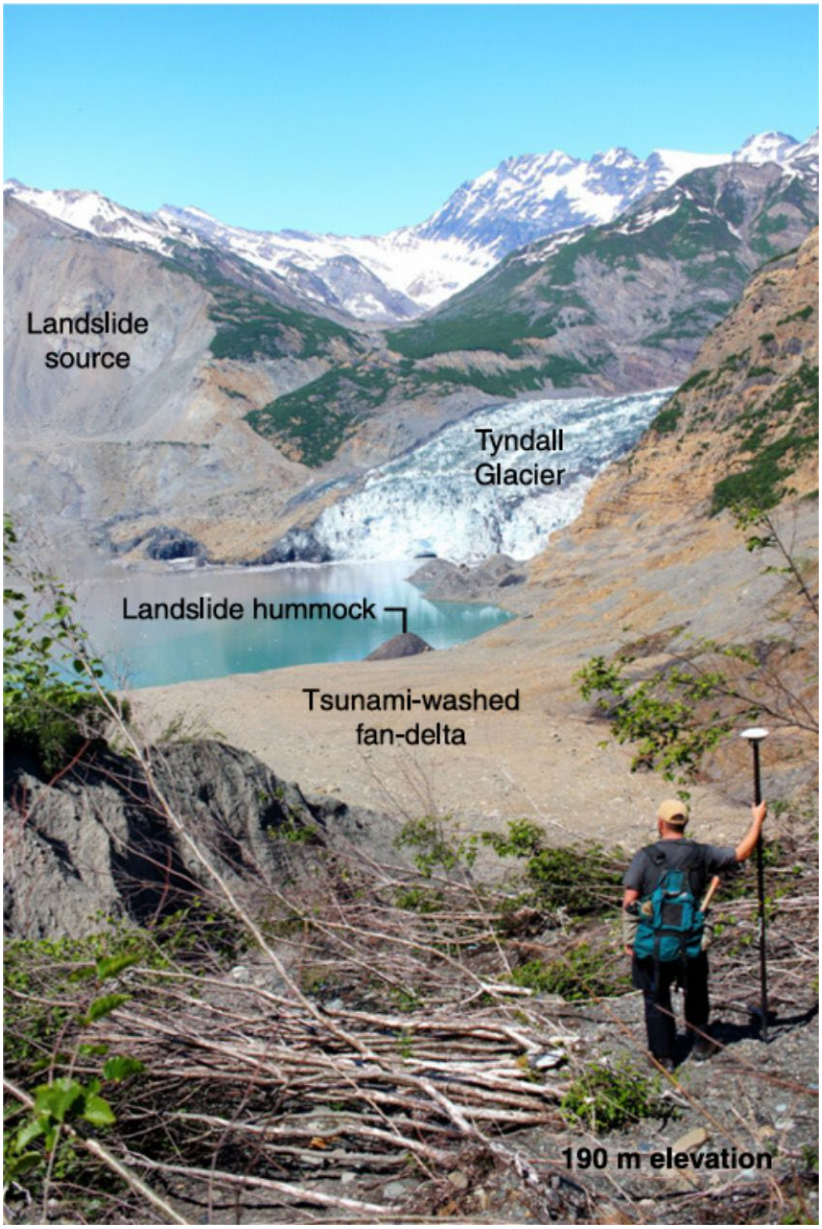


Figure 5. Tsunami impacts near the Taan Fjord landslide. The 2015 landslide and tsunami reshaped the landscape at the terminus of the Tyndall Glacier. The person in the photo is standing about 190 m above the fjord level, just below the limit of inundation. (From *Higman et al.* [2018]).

Rapid climatic warming over the last 50 years has led to a 17 km retreat of the ice terminus and 400 m ice thinning of the Tyndall Glacier [*Higman et al.*, 2018; *Haeussler et al.*, 2018]. The slope that failed was above the calving terminus front. The onshore scars, destruction of forest and vegetation and other tsunami marks help delineate tsunami runups along the fjord. The maximum runup of 193 m occurred on 17 October 2015, when a massive tsunami occurred

directly across from the landslide (Figure 6). For about 1.5 km from the slide area, tsunami runup exceeded 100 m. It subsequently deminished to about 15 m at the mouth of the fjord, located about 17 km from the source area at the head of the fjord (Figure 6) [*Higman et al.*, 2018]. As was indicated by the authors: *While the 2015 Taan Fjord landslide and tsunami did not result in fatalities, actively deforming slopes in more populated places (e.g. Tidal Inlet, Glacier Bay National Park, Alaska24) may be harbingers of more deadly landslide-generated tsunamis in the future. Monitoring gradual downslope motion in mountain ranges around the world, while a technical challenge, would provide a step forward in our ability to mitigate risk.*

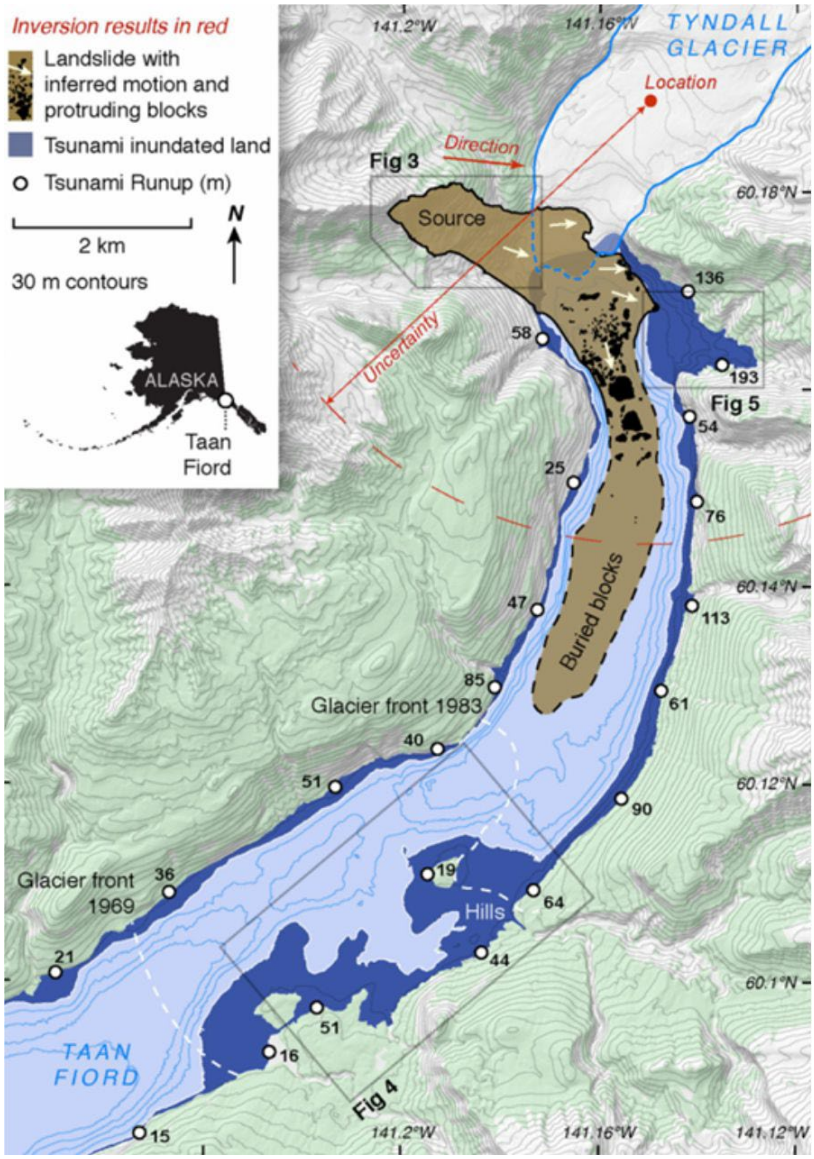


Figure 6. Changes in Taan Fjord. The Tyndall Glacier retreated at an increasing pace through the late 20th century until it stabilized in 1991. The slope failure in October 2015 entered the recently deglaciated fjord at the calving front, generating a major tsunami that swept the shoreline to a height of 193 m. In 2016, marine surveys revealed tens of meters of thick blocky submarine runout extending several kilometers. Map created with QGIS 2.18 (http://www.qgis.org/en/site/) (From *Higman et al.* [2018]).

3. TRACY ARM LANDSLIDE AND TSUNAMI

Tracy Arm is located about 200 km southeast of Juneau (Figure 7). At 13:26 UTC (05:26 AKDT) on 10 August 2025, a large rockface located above the toe of the South Sawyer Glacier fell into the fjord, producing a gigantic tsunami that was recorded by the NOAA tide gauge at Juneau. This was second largest tsunami ever recorded after the 1958 Lituya Bay tsunami (described in Section 2.2), but no injuries or fatalities were reported [*Toney et al.*, 2025]. The event attracted much scientific and public attention.

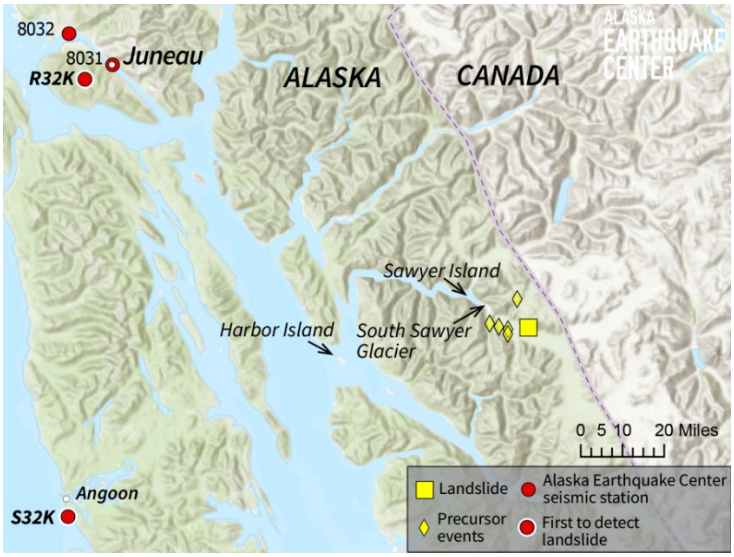


Figure 7. Map of the 2025 Tracy Arm landslide location and the precursory events detected in the seismic record. The red circles show the Earthquake Center's seismic stations in the region. Station S32K near Angoon and R32K near Juneau were the first to detect the landslide. Harbor Island is where several kayakers lost their gear to the tsunami. Sawyer Island is where reports indicate a tsunami of 30 m scraped trees off the rocky slopes. (From *Grassi and Karasozen* [2025]; https://earthquake.alaska.edu/major-landslide-southeast-alaska-fjord).

Initial information on the event came from the Alaska Earthquake Center (AEC) [*Boyce*, 2025; *Grassi. and Karasözen*, 2025], which detected a seismic signal that was almost certainly generated by a landslide. *Karasözen and West* [2024] had previously developed a method to remotely detect large landslides within minutes of occurrence and to quickly determine whether the slides are close to open water and present a tsunami hazard. The Center's preliminary analysis, based on this method, estimated the landslide's volume to be larger than 10^8 m^3, 30 times that of the 2020 Elliot Creek landslide. As emphasized by Michael West, the AEC Director, "*This is larger than anything in the past decade in Alaska. It's going to get a lot of attention from*

scientists… Holy Grail of hazard monitoring". The importance of this event was also highlighted by Dave Petley in an EOS information article [*Petley*, 2025].

Eyewitness reports provided first hand information on the local displacement wave [*Petley*, 2025]:

"Kayaker Sasha Calvey said she and two others were camping on Harbor Island in Tracy Arm Inlet, a fjord about 45 miles south of Juneau (sic), when a landslide or iceberg caused a tidal surge that swept away half of their gear, including one boat, personal items, and cooking equipment. Calvey said their gear had been stored about 25 feet above the high tide line, but the water reached it and came within an inch of sweeping away their tent. She added that they placed a radio distress call that was picked up by a boat, which transported them to Juneau."

The USGS, based on the information from the AEC, operatively reported about the event and published a map showing the location of the slide area (on the north side of the fjord containing South Sawyer Glacier) and the position of Harbor Island (about 60 km from the slide), where Sasha Calvey observed the tsunami wave (Figure 8) [*Toney et al.*, 2025]:

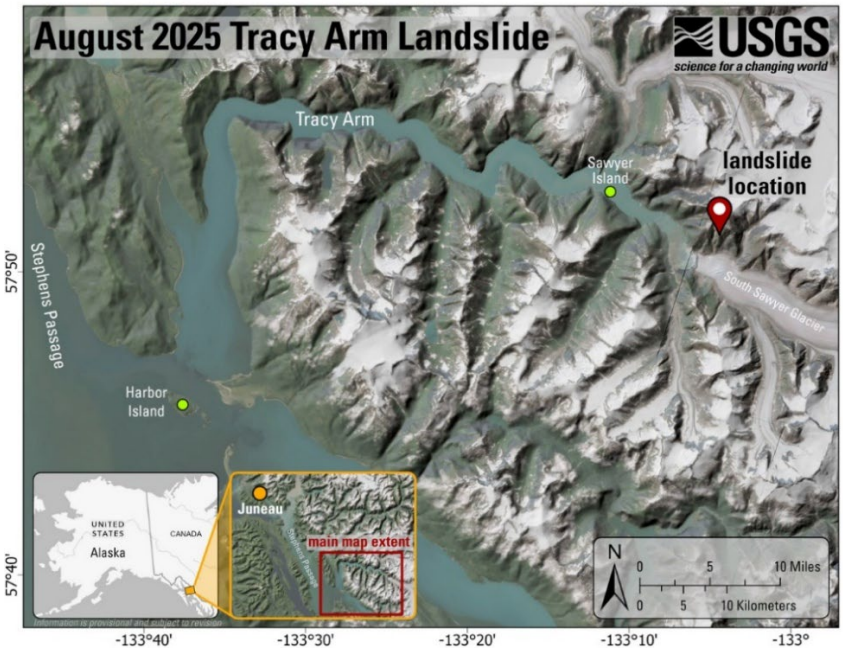


Figure 8. Overview map and location of the Tracy Arm landslide-generated tsunami event. The imagery is not current**;** the South Sawyer Glacier has retreated over a kilometer from what is depicted. (From *Toney et al.* [2025]; https://www.usgs.gov/programs/landslide-hazards/science/2025-tracy-arm-landslide-generated-tsunami).

Preliminary interpretation of photos taken by kayakers in the area indicates that the landslide generated a tsunami at least 30 meters high at Sawyer Island (Figure 8), a small island located where the fjords containing South Sawyer and North Sawyer glaciers meet. The tsunami was also recorded far from the landslide by a NOAA coastal tide gauge in Juneau; the Alaska

Earthquake Center reported that the maximum tsunami wave height at the gauge was 36 cm above the tide, and that the waves continued for hours [*Toney et al.*, 2025].

The AEC continued to examine the event and collect various information in the period that followed [*Boyce*, 2025]. As Ezgi Karasözen noted: "*We were able to produce a rapid location and volume estimate using seismic data as soon as we learned about the event*". Heather McFarlin, the center's seismic data manager, said the landslide's energy release was approximately equivalent to that from a magnitude 5 earthquake. "*This may be the best-documented example of such precursors, which gives us real motivation to explore precursor detection in addition to ongoing monitoring*," Karasözen said. "*That will likely be a focus for us going forward.*".

Figure 9 shows the seismic records within a thousand kilometers from the Tracy Arm landslide examined by the AEC (https://earthquake.alaska.edu/event/025a7d7cil/detail). The stations located close to the landslide source area recorded the signal first. At greater distances, the seismic waves arrived later and the signal more protracted. The amplitudes of these seismic signals hundreds of kilometers from the source were used to estimate the volume of the landslide.

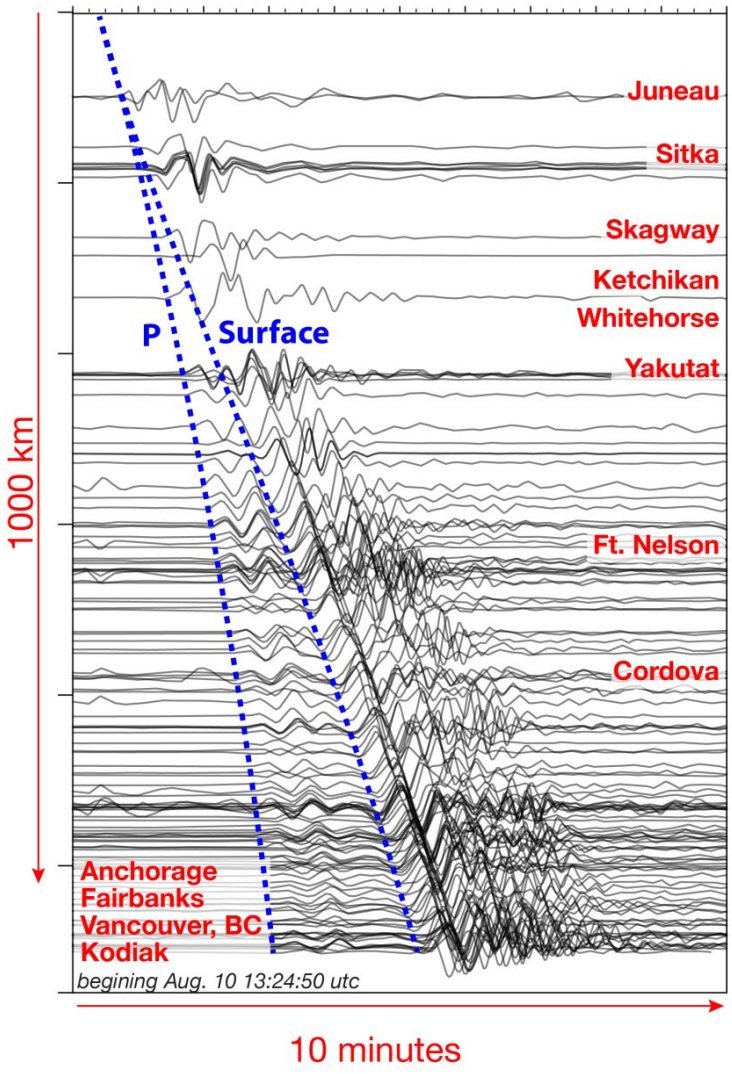


Figure 9. Seismic records of the Tracy Arm landslide from stations located within a thousand kilometers of the Tracy Fjord landslide. (From AEC (2025]; https://earthquake.alaska.edu/event/025a7d7cil/detail).

The AEC [2025] also compared the seismic signals from two events: the 2015 Taan Fjord landslide (see Section 2.3) and the 2025 Tracy Arm landslide. This side-by-side comparison is shown in Figure 10. Volume estimates depend on the landslide height and run-out, as well as the mass of the material. In the case of the 2015 Taan Fjord slide, the volume was estimated to be 70-80 million m^3. The results presented in Figure 10 clearly indicate that the 2025 Tracy Arm slide had a significantly greater volume well in excess of 100 million m^3.

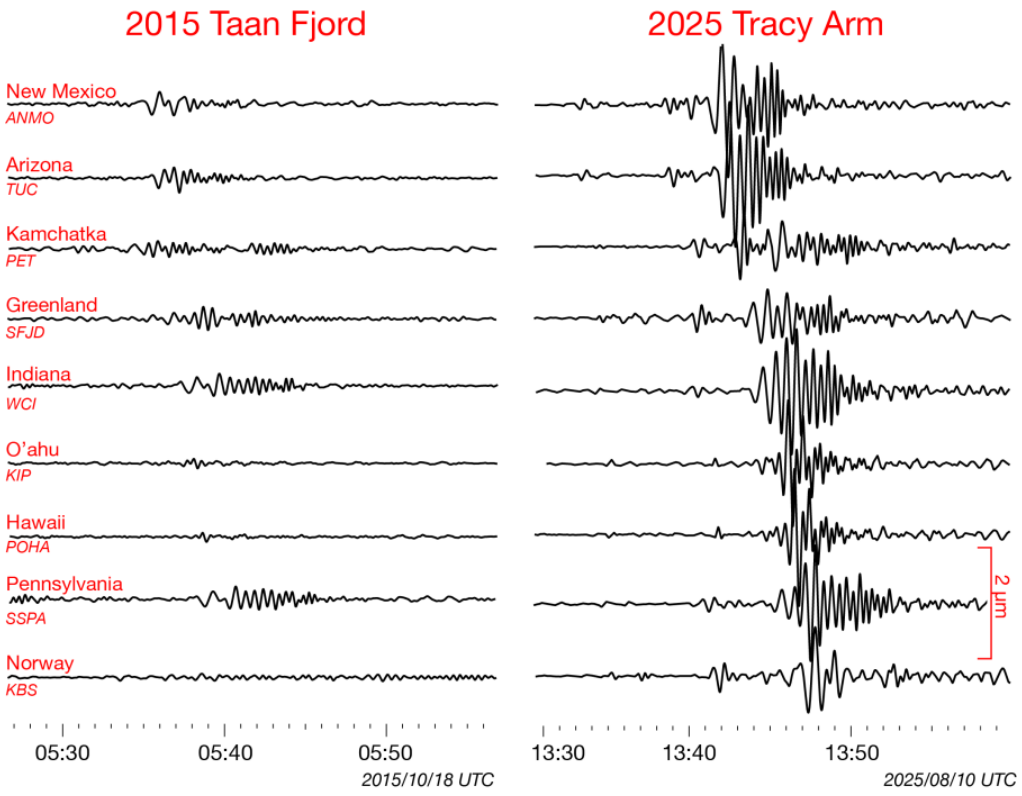


Figure 10. A side-by-side comparison of seismic records from the 2015 Taan Fjord and 2025 Tracy Arm landslides. The seismograms are the vertical component (BHZ) records from stations in the Global Seismographic Network at distances of 3200 to 4600 km from the source. Records are filtered for periods between 20 to 100 sec and corrected for instrument response. (From the *Alaska Earthquake Center* [2025]; https://earthquake.alaska.edu/event/025a7d7cil/detail).

The U.S. Coast Guard made the first helicopter examination of the Tracy Arm event. Dr. Michael West of the American Earthquake Center (AEC) used the Coast Guard's video from the flyover to examine the landslide : https://www.youtube.com/watch?v=mrZ9VRfAW-k. (Coast Guard video credit: LT Chip Baucom and CDR PJ Johansen, U.S. Coast Guard.).

A satellite image acquired by the USGS on August 13th several days after the landslide (Figure 11) clearly shows the slide location on the north side of the fjord containing South Sawyer glacier. The landslide material appears to have directly entered the water adjacent to the terminus of the glacier. Preliminary estimates indicate a volume of up to ~100 × 10^6 m^3.

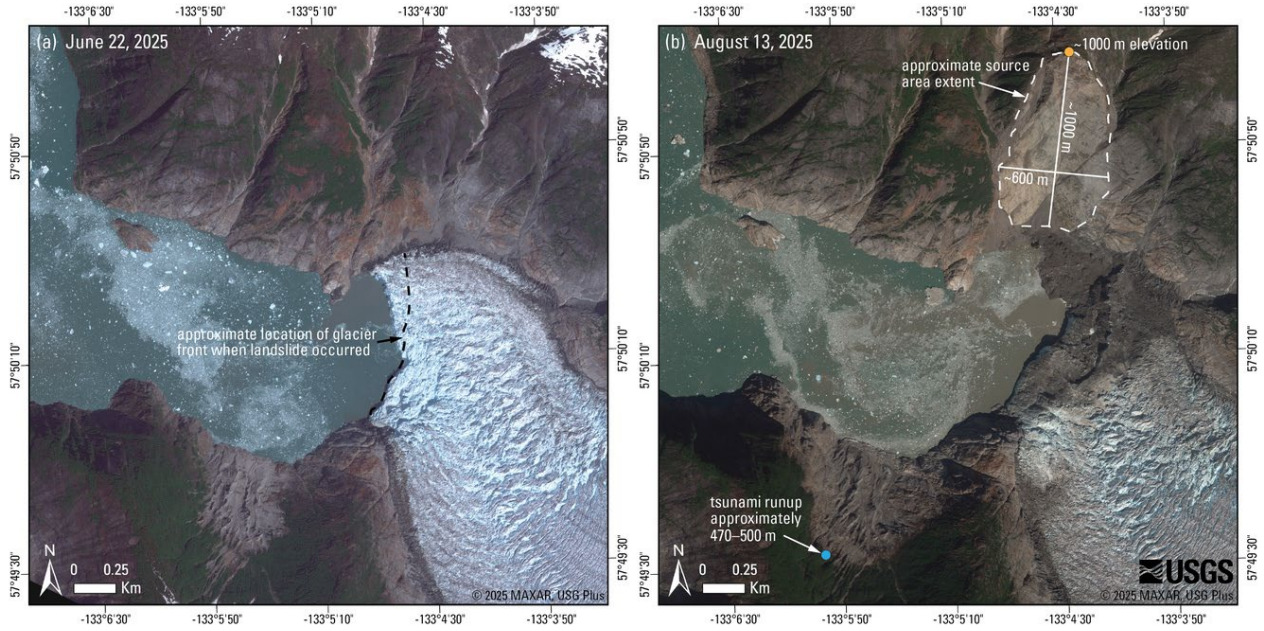


Figure 11. Comparison of (a) pre- and (b) post-event satellite images showing the source area of the Tracy Arm landslide of 10 August 2025. The dashed line in (a) shows the approximate location of the leading edge of the South Sawyer Glacier on 7 August 2025 (mapped from imagery © 2025 Planet Labs PBC). Part (b) shows the approximate extent of the landslide source area, the area of the South Sawyer Glacier that was impacted by the landslide, and the approximate extent of tsunami runup on the opposite side of the fjord. Pre- and post-event images are from 22 June and 13 August 2025, respectively. Imagery © 2025 Maxar, USG Plus. Approximate headscarp and tsunami runup elevations were measured from a 5 m-resolution interferometric synthetic aperture radar (IFSAR) digital elevation model (DEM) collected in 2012. (From: *Toney et al.* [2025]).

On August 13th, USGS personnel conducted a helicopter-borne aerial survey of the area. A few characteristic photos are shown in Figures 12 and 13. Satellite and digital elevation model analysis indicate a runup height of approximately 470–500 m opposite the landslide (*Toney et al.* [2025]) . The results we present in this section are based on the first study of the event. More detailed and precise analyses of this event in scientific papers presently in press.



Figure 12. (a) Oblique aerial photo of the 10 August 2025 Tracy Arm landslide source area captured during a field reconnaissance overflight on 13 August 2025; (b) A landslide photo taken from across the fjord during the field reconnaissance overflight on 13 August 2025. Both photos are looking approximately to the north. (From: *Toney et al.* [2025]).



Figure 13. (a) Oblique aerial photo of the 2025 Tracy Arm landslide and South Sawyer Glacier captured during a field reconnaissance overflight on 13 August 2025. The image is looking toward the southeast; (b) Photo of tsunami-inundated shoreline at Williams Cove, near the mouth of Tracy Arm. The image is looking approximately to the north (From: *Toney et al.* [2025]).

3A. TIDE GAUGE OBSERVATIONS

In order to detect the signal from the 2025 Tracy Arm landslide tsunami, we used the water level records from six National Oceanic and Atmospheric Administration (NOAA) coastal tide gauges (TG) and six Canadian Hydrographic Service (CHS) tide gauges (locations are shown in

Figure 14). With the exception of the NOAA gauge at Juneau, which had a sampling interval, Δt = 6 min, all instruments had a relatively high sampling interval of 1 min. Unfortunately, it was the Juneau gauge that was the closest to the landslide source area and, therefore, of greatest interest for our study.

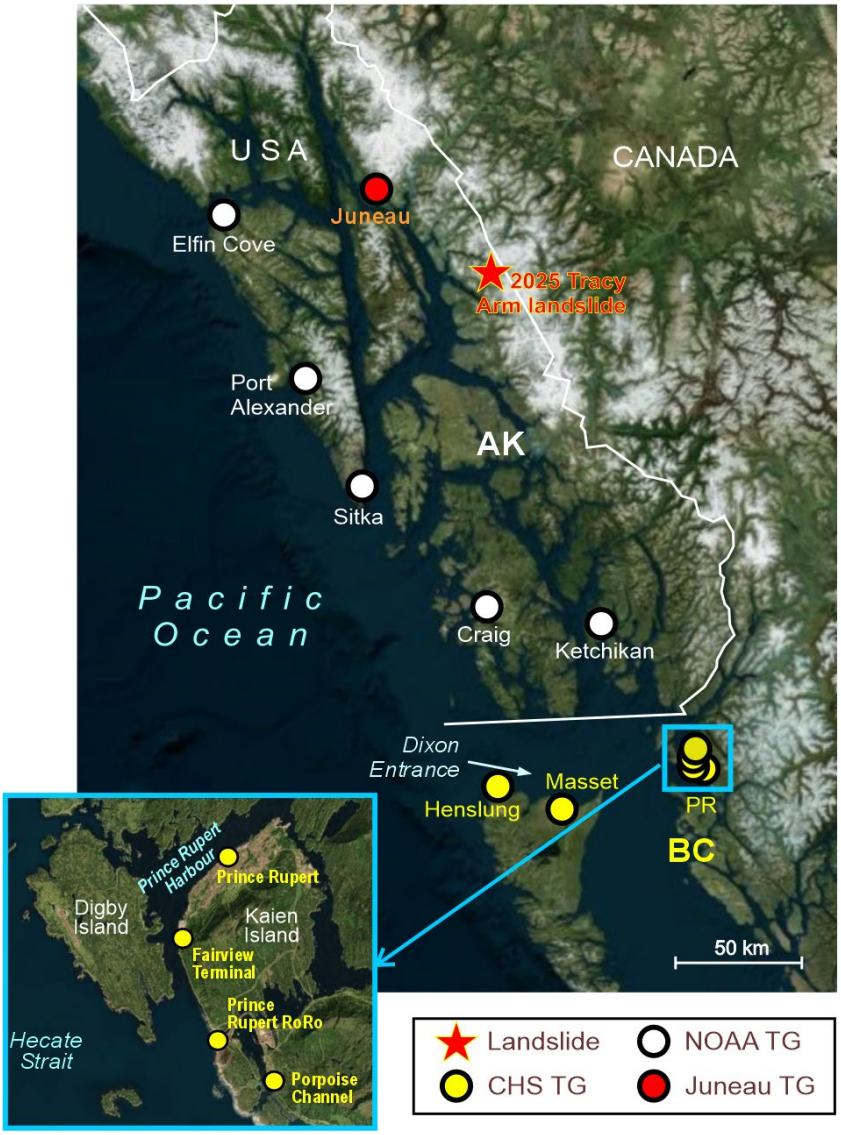


Figure 14. Map of southeastern Alaska (AK) and northern British Columbia (BC) showing locations of the NOAA (white circles) and CHS (yellow circles) tide gauges (TGs); the locations of the Prince Rupert group of CHS tide gauges are shown in the inset. The red circle indicates the Juneau NOAA tide gauge that clearly recorded the Tracy Arm landslide tsunami. The sampling interval for Juneau was 6 min; all other records had 1-min sampling. The red star denotes the location of the landslide.

The TG records have been examined using data analysis procedures described by *Rabinovich and Stephenson* [2004] and *Rabinovich et al.* [2013]. Specifically, the data were first verified and corrected; gaps were then filled, spikes removed and the timing checked. The tides for the CHS

records were calculated and subtracted from the original records (the NOAA tide gauge records were already de-tided by the National Centers for Environmental Information (NCEI)). The residual time series formed the basis for further analysis. To suppress low-frequency sea level variations, mostly associated with atmospheric activity, we further applied a high-pass filter with a 3-h Kaiser-Bessel (KB) window to the residual time series [cf. *Thomson and Emery*, 2024].

3B. RESULTS

Figure 15 presents 1.5-day duration, de-tided and high-pass filtered records from the six NOAA tide gauges shown in Figure 14 for the period of 10-11 August 2025. The tsunami wave was observed to arrive at the Juneau station at 14:12 UTC, i.e., 48 min after the Tracy Arm landslide. The amplitude of the first wave relative to undisturbed sea level was about +26 cm. The crest of the second wave was relatively small, +8.2 cm, but the corresponding trough semi-wave was the largest, -28.7 cm. The maximum amplitude of +27.6 cm was attained during the fourth wave, which was recorded at 15:30 UTC (1 h 18 min after the first wave arrival). The overall range of the measured tsunami waves – the difference between the maximum trough and the maximum crest - was 56.3 cm. After the arrival of the highest wave (the 4^{th} wave), the tsunami amplitudes began to decrease gradually. The total tsunami ringing lasted for about 8 hours (Figure 15).

It should be noted that the relatively long sampling interval at station Juneau (Δt = 6 min) strongly affected the resulting wave parameter estimates in that the real tsunami amplitudes were probably 50% higher than those recorded. Also, we do not know the actual periods of the generated tsunami waves but it is likely that they were much shorter than the period of 20 min recorded at this station (Figure 16). Theoretically, the period of generated tsunami waves is determined by the horizontal dimensions of the source area and the local water depth. Typical dimensions of the earthquake sources are from several tens to a few hundred kilometers; the landslide source areas are one-two orders smaller. Accordingly, typical periods of landslide tsunamis are one-two orders shorter than those of seismic tsunamis. Thus, the periods of the Tracy Arm generated tsunami waves near the source area (i.e., before they began to be strongly transformed by topographic features) were likely only a few minutes, or even shorter.

No tsunami waves were detectable at the five other NOAA stations (Figure 15); either the waves generated in Tracy Arm attenuated very rapidly with distance or these stations were well sheltered from the incoming waves.

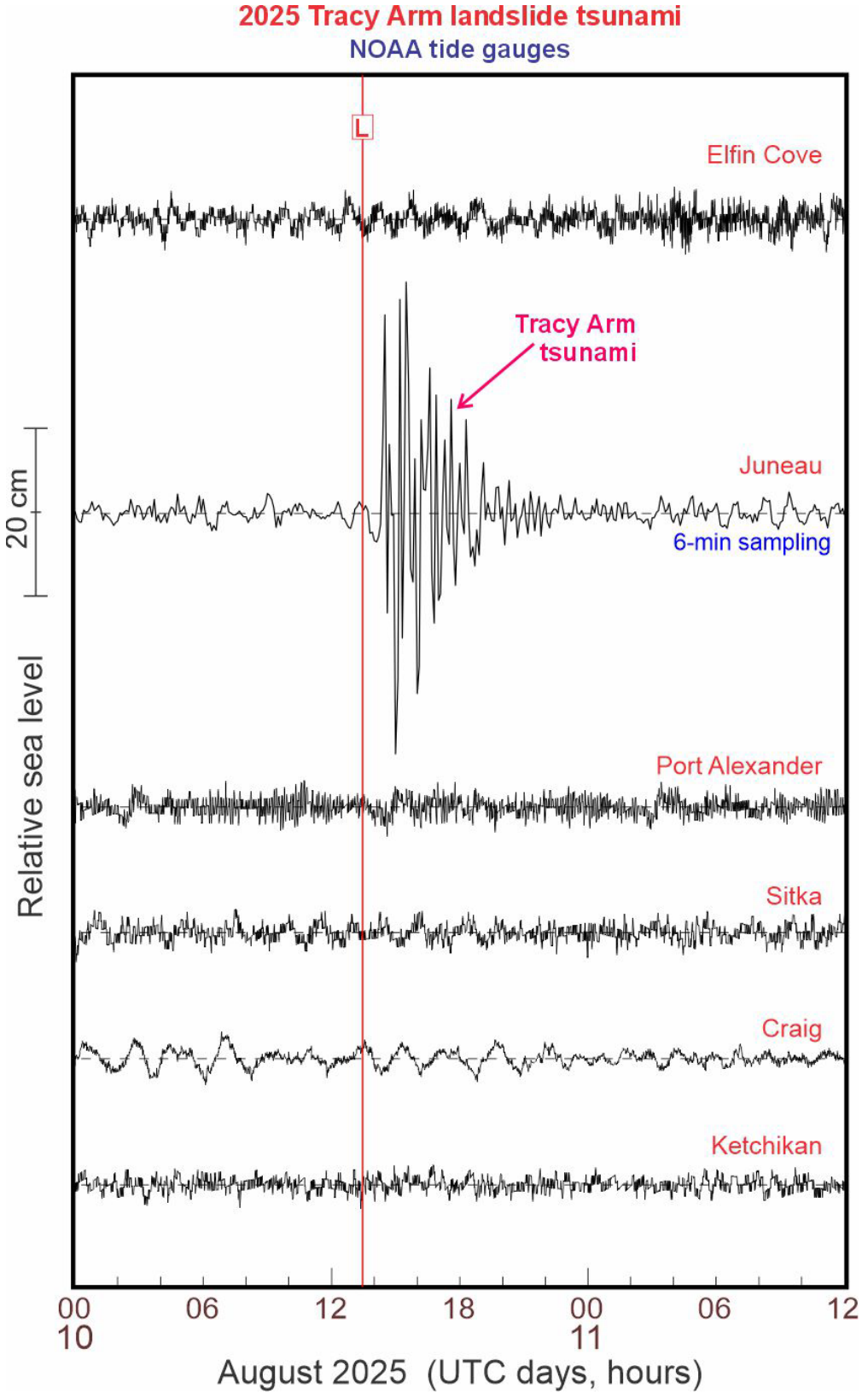


Figure 15. De-tided and high-pass filtered (3-hour Kaiser-Bessel window) 1.5-day duration NOAA tide records for the time of the 2025 Tracy Arm event. The solid vertical red line labelled "L" indicates the time of the landslide. The individual records are shifted in the vertical relative to each other. The tsunami signal is evident in the record of Juneau but not in the other records.

To examine temporal variations of high-frequency sea level fluctuations in the tsunami frequency domain and to estimate the dominant periods of recorded oscillations at various sites, we used a multiple-filter method, which is similar to wavelet analysis [cf. *Thomson and Emery*, 2024]. This method has been effectively applied previously to investigate various tsunami events [cf. *Rabinovich et al.*, 2013, 2017, 2025; *Zaytsev et al.*, 2017] and enables determination of the evolution of propagating waves as a function of frequency, f, and time, t. The resulting $f-t$ diagrams display possible nonstationary properties of the observed waves, which in turn help identify some masked tsunami waves, waves that are not seen in the records themselves (probably because of high level of background noise), but which can be revealed by abrupt changes in the frequency content.

The $f-t$ diagrams for the six NOAA stations are displayed in Figure 16. The tsunami signal is obvious in the $f-t$ diagram for station Juneau. In addition to the dominant period of 20 min, the analysis reveals motions at a period of 60 min. The latter period is likely associated with the fundamental (Helmholtz) period of Tracy Arm fjord. For the five other $f-t$ diagrams, there are no oscillations that can be associated with tsunami waves. Thus, both inspection of the records (Figure 15) and their $f-t$ diagrams reveal that Juneau was the only station that recorded the 2025 Tracy Arm tsunami.

The above analysis procedure (record inspection and $f-t$ analysis) was also applied to the six Canadian CHS tide gauge records (Figures 17 and 18). But neither in the records themselves, nor in their $f-t$ diagrams are there any signatures of tsunami waves. In the $f-t$ diagrams for two stations, Prince Rupert Ro Ro and Porpoise Channel, there were oscillations with periods of about 15-20 and 60 min that began at about 13:50 UTC (Figure 18), i.e., about 25 min after the landslide. However, this is too early for the tsunami signal to arrive (the waves needed at least 2.5-3 hours to reach these two sites), forcing us to conclude that the 2025 Tracy Arm landslide tsunami waves did not reach the coast of British Columbia.

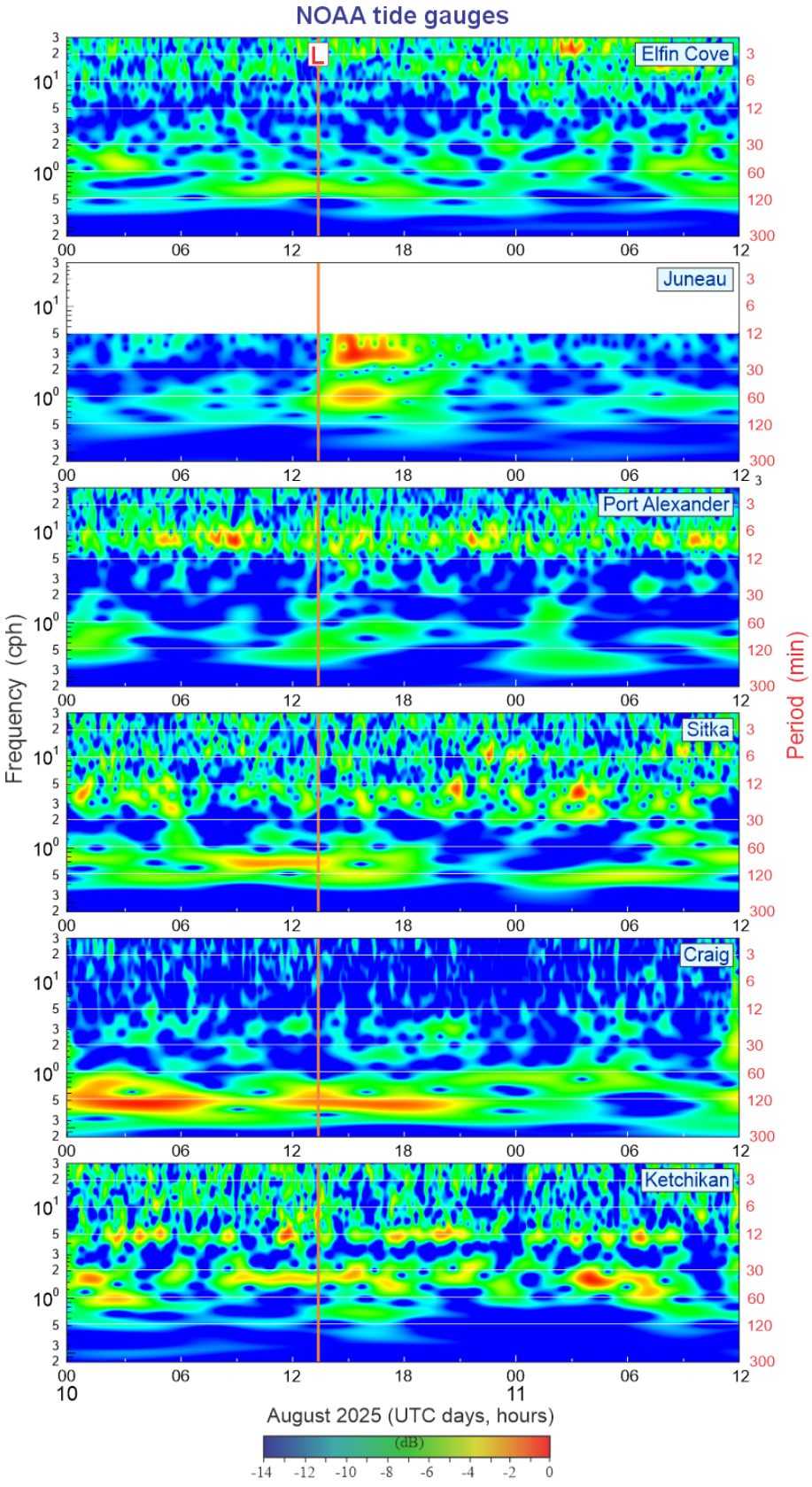


Figure 16. Frequency–time plots (*f–t* diagrams) for the six NOAA tide-gauge records shown in Figure 15. The solid vertical red lines labelled "L" indicate the time of the 2025 Tracy Arm landslide. The Juneau record had a 6-min sampling, whereby the frequency band examined for this station was 0.2 – 5 cph; for the five other stations, the band was 0.2 – 30 cph.

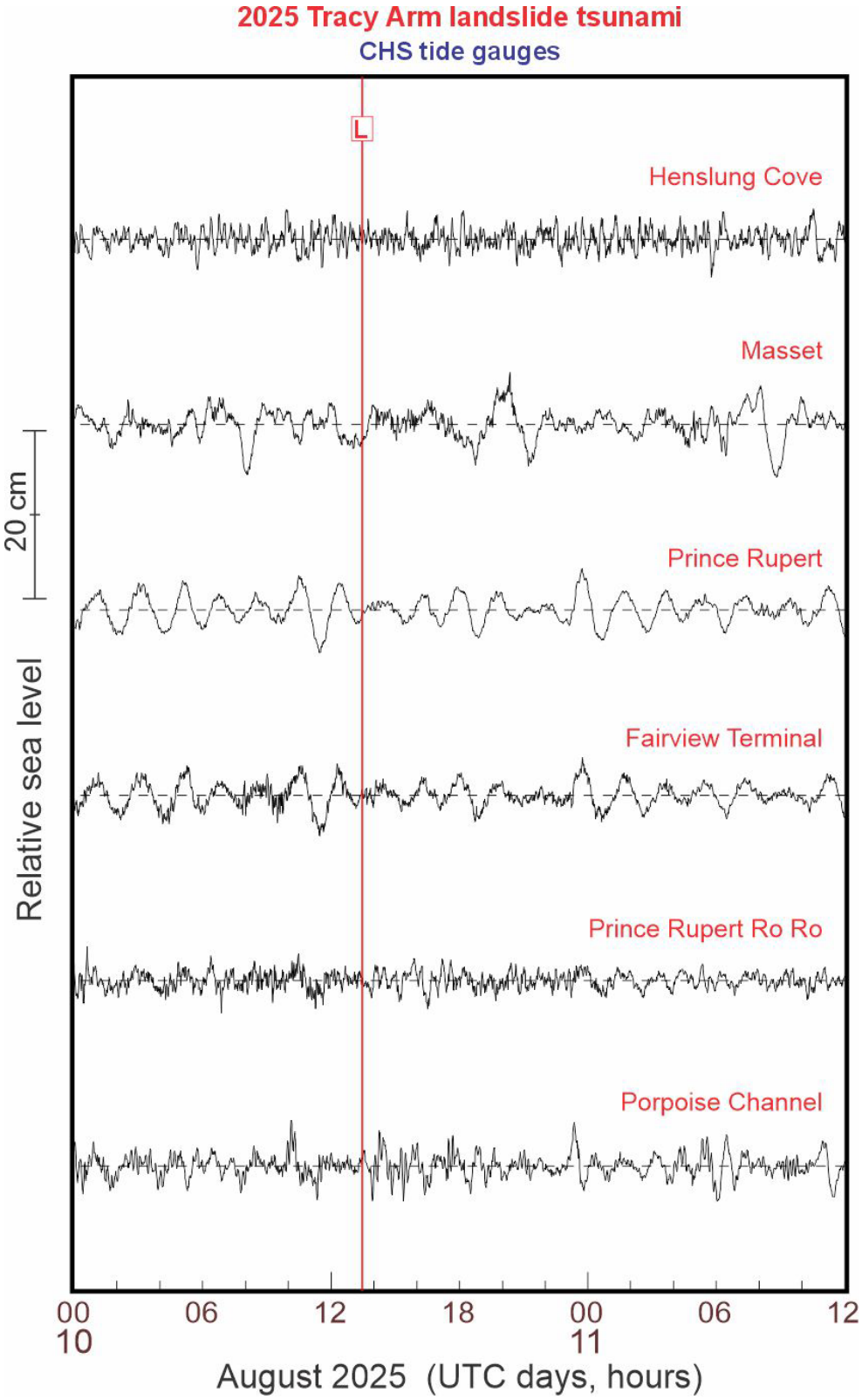


Figure 17. De-tided and high-pass filtered (3-hour Kaiser-Bessel window) 1.5-day duration CHS tide record segments for the time of the 2025 Tracy Arm event. The solid vertical red line labelled "L" indicates the time of the landslide. The individual records are shifted in the vertical relative to each other.

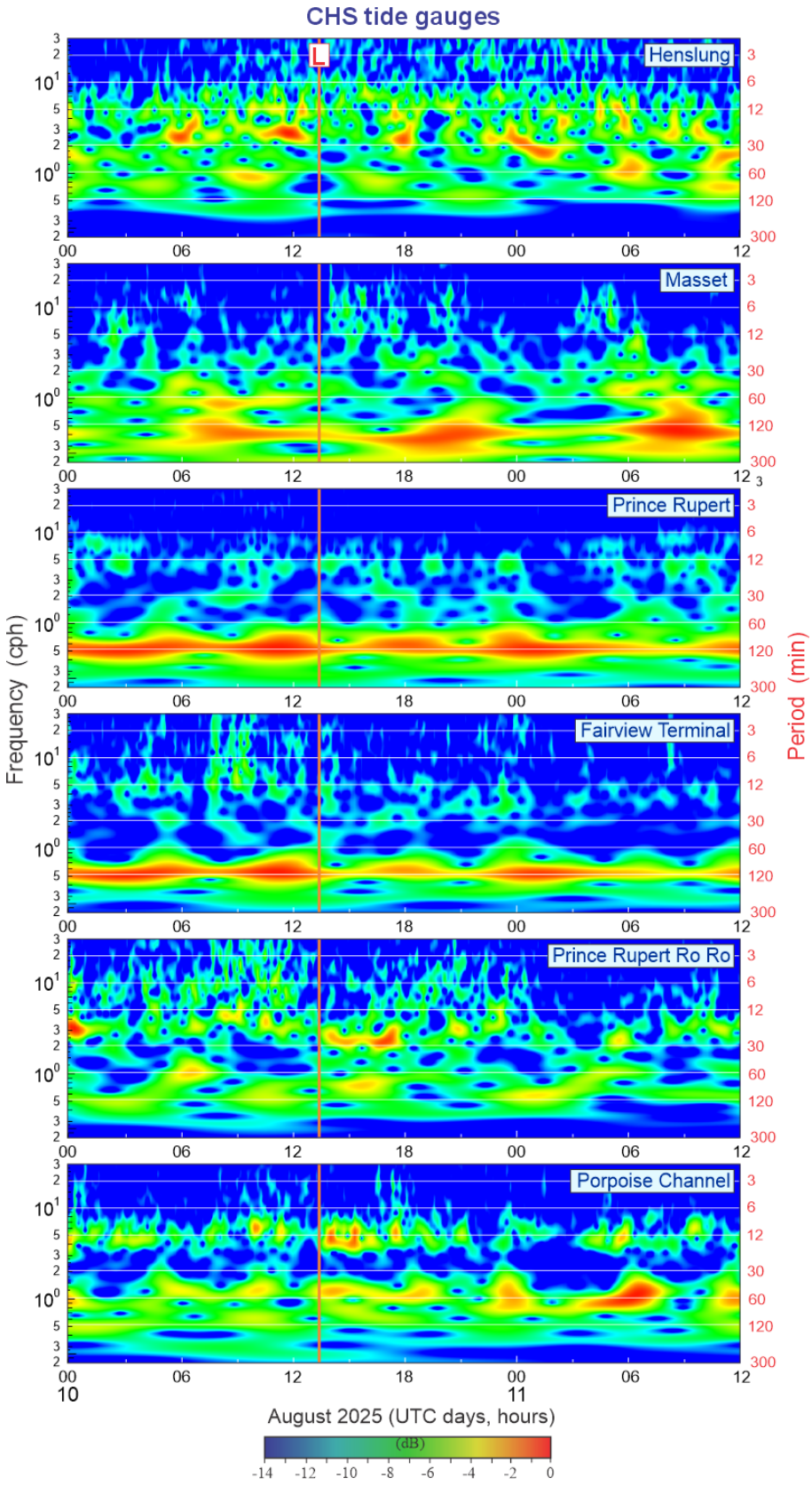


Figure 18. Frequency–time plots (*f–t* diagrams) for the six CHS tide-gauge records shown in Figure 17. The solid vertical red lines labelled "L" indicate the time of the 2025 Tracy Arm landslide.

4. SUMMARY AND CONCLUSIONS

Landslides and associated tsunamis present a very serious threat for the Pacific coast of North America. Although landslide-generated tsunamis are typically more localized than seismically generated tsunamis, they can produce destructive coastal runups and cause severe damage. Landslides, slumps and rockfalls are often the secondary effects of earthquakes. However, in many cases, damaging submarine landslides are produced by local processes in the absence of seismic events. The sudden deposition of sediment loads in deltaic areas, slope erosion, construction-related loads and activity, as well as meteorological factors such as rainfall, strong winds, and abrupt atmospheric pressure change, are common triggers of slope failures.

The present report provides an overview of several strong landslides and associated tsunamis that have occurred on the coasts of British Columbia and southeastern Alaska. Specific attention is given to three events: (1) the Kwalate historical event (~1570 AD); (2) the gigantic 1958 Lituya Bay event; and (3) the major 2015 Taan Fjord event. In many respects, the physical mechanisms and the character of these three events are similar to those of the 2025 Tracy Arm landslide and tsunami, the main focus of our study.

The roughly 100 million cubic meter Tracy Arm landslide produced gigantic tsunami waves with a maximum runup height of 470-500 m, the second largest after the 1958 Lituya Bay tsunami (525 m). Fortunately, no one was injured or killed by the event. However, as was emphasized by *Higman et al.* [2018] about the 2015 Taan Fjord landslide *"…actively deforming slopes in more populated places (e.g. Tidal Inlet, Glacier Bay National Park, Alaska24) may be harbingers of more deadly landslide-generated tsunamis in the future. Monitoring gradual downslope motion in mountain ranges around the world … would provide a step forward in our ability to mitigate risk."* The same can be said about the 2025 Tracy Arm event. One of the important lessons arising from this event is the necessity for a thorough examination and modelling of possible submarine sliding/slumping and slide-generated tsunamis in areas of existing and new construction, especially in the vicinity of unstable sediment accumulations.

For this study, we collected and examined all available information about the 2025 Tracy Arm event, including photos, videos and satellite images. We also thoroughly examined the data from six NOAA tide gauges located in the relative vicinity of the event and six CHS tide gauges located in northern British Columbia. The tsunami signal was evident at only one gauge site: station Juneau, the closest to the landslide source area. According to the seismic records, the Tracy Arm landslide occurred at 13:26 UTC on 10 August 2025. The first tsunami wave arrived at Juneau at 14:12 UTC, i.e., 48 min after the event. The maximum recorded tsunami amplitude

was 27.6 cm, while the maximum trough-to-crest range was 56.3 cm. It should be noted that during the time of the event, station Juneau was operating with a sampling interval of 6 min, which is not sufficiently rapid to reliably measure parameters of tsunami waves, especially relatively high-frequency waves such as those associated with landslides. The actual tsunami amplitudes at this station were probably about 1.5 times higher than recorded.

No tsunami signal was detected at the 11 other stations, including 6 stations located in northern British Columbia. This demonstrates that landslide generated tsunamis, even so gigantic as the 2025 Tracy Arm tsunami, typically have a local character and do not propagate far away from the source area. At the same time, this event shows the necessity to have much better spatial resolution of the instruments in the high-risk regions and higher time/height resolution of these instruments.

5. SUPPLEMENT: *Science* publication on the Tracy Arm landslide and tsunami

After the present report had been completed, the first scientific publication on the Tracy Arm appeared: "*A 481-meter-high landslide-tsunami in a cruise ship–frequented Alaska fjord*" by *Shugar et al.* [2026]. The published Abstract follows:

Abstract: *Early in the morning of 10 August 2025, a >64×10^6 m^3 landslide struck Tracy Arm fjord in Alaska. The landslide was preconditioned by glacial retreat caused by climate change. The resulting* ***481 m runup*** *megatsunami followed an initial 100-m-high breaking wave traveling >70 m/s. The landslide was preceded by several days of microseismicity, which increased in rate and magnitude until ~1 hour before failure. The landslide produced globally observed long-period seismic waves equivalent in size to a M5.4 earthquake. A long-period (~66 s) global seismic signal, produced by a landslide-induced seiche trapped within the fjord, persisted for up to 36 hours, the second time a days-long seiche has been thus observed. With fjord regions increasingly visited by cruise ships, and climate change making similar events more likely, this unanticipated, near-miss event highlights the growing risk from landslides and tsunamis in coastal environments.*

The findings in the *Science* paper made it possible for us to specify the parameters of this extraordinary event. In particular, it was estimated that the maximum tsunami runup occurring on the south side of the fjord, in ~3.3 km across from the landslide headscarp, was **481±7.6 m**. These estimates were obtained from a helicopter-mounted altimeter.

In addition to the record at the NOAA tide gauge at Juneau (station ID 9452210), which was used in the present study (Figure 15), the authors of the Science paper also used a gauge operated by JOA Surveys with NOAA support (station ID 9452005) that recorded the tsunami wave in Endicott Arm, Alaska, about 130 km (tsunami travel distance) from the source area. This

gauge measured a tsunami peak amplitude of 0.4 m with the initial crest arriving 1 hour after the landslide. Key results of *Shugar et al.* [2026] are presented in Figures S1 and S2.

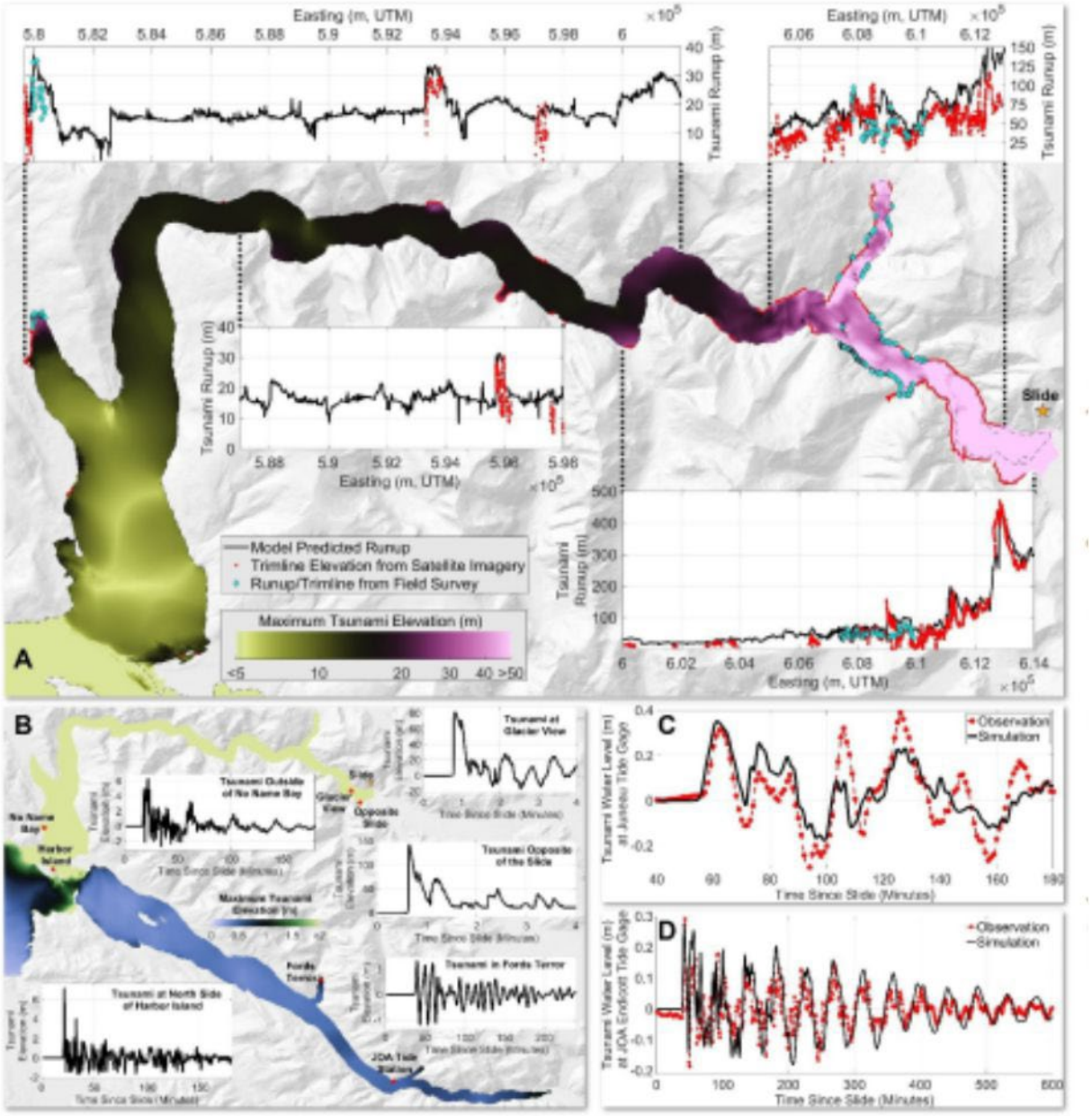


Figure S1. Summary of the tsunami simulation - observation comparisons. (A) Tsunami elevations and runup in Tracy Arm. The maximum tsunami elevations from the numerical model are shown in the map view, with red lines indicating the locations of tsunami trimlines from satellite imagery and the light blue diamonds indicating the runup measured during the field survey. The inset panels above and below provide comparisons between the model-predicted runup (black lines) and the satellite-inferred trimline/runup (red dots/blue diamonds) along the northern and southern shorelines of Tracy Arm, respectively. (B) Tsunami simulation results for Tracy Arm and Endicott Arm. Time series of the tsunami elevation are shown from various locations indicated by the red stars. (C) Model (black line) comparison with the tide gauge data (red dots) from the NOAA Juneau tide gauge, which records sea levels every 1 min. (D) Model (black line) comparison with the JOA tide gauge data (red dots) from Endicott Arm, sampled every 1 min (from *Shugar et al.* [2026]).

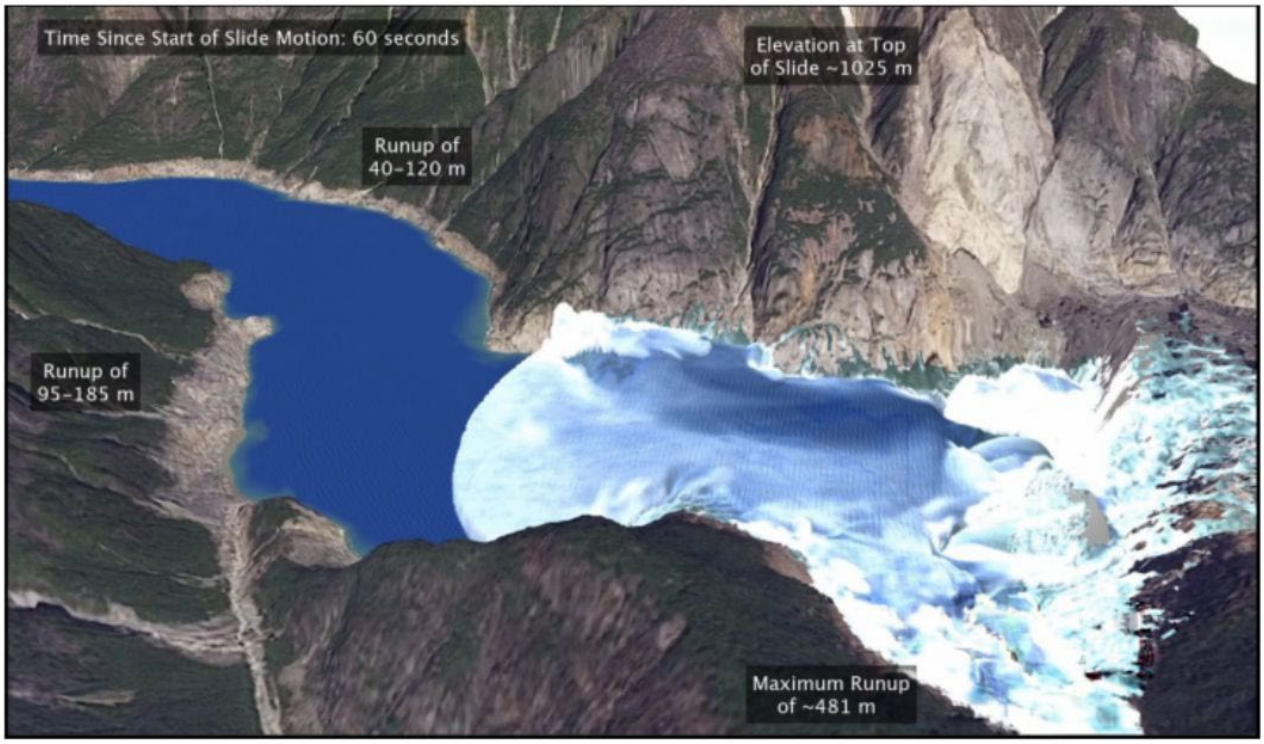


Figure S2. Snapshot from a near-source animation of the tsunami generated by the Tracy Arm landslide. The tsunami is shown with a photorealistic render and the post-event Planet SuperDove satellite imagery draped over topography. Runup values are satellite-derived trimline elevations. Animations in the Science publication begin with a perspective view of the landslide- and tsunami-impacted areas, shown at a time before the landslide has started to move and then when roughly ¾ of the landslide volume is in the water and a large breaking tsunami with crest elevation of 125 m has been generated. At 90 s, the tsunami runs ≥150 m up a slope 3 km from the landslide. The tsunami continues down Tracy Arm, with strong amplification along a southern shoreline river mouth with maximum runup near 150 m, before reaching Sawyer Island 3.5 min after the start of landslide motion. At the island, the tsunami energy splits, with energy continuing to the west in the main Tracy Arm channel and energy traveling northward toward Sawyer Glacier, where runup elevations again exceed 100 m. (from *Shugar et al.* [2026]).

ACKNOWLEDGEMENTS

The authors acknowledge the help of George Mungov (National Centers for Environmental Information NOAA, Boulder, CO) in the preparation of the tide gauge time series, which were used to identify and examine the Tracy Arm tsunami signal, and the help of Elena Suleimani (University of Alaska, Fairbanks) in the collection of information on the 2025 Tracy Arm landslide and tsunami.

REFERENCES

Alaska Earthquake Center, AEC (2025). *2025 Tracy Arm Landslide*, University of Alaska Fairbanks, https://earthquake.alaska.edu/event/025a7d7cil/detail

Bornhold, B., Harper, J., McLaren, D., and Thomson, R. (2007). Destruction of the First Nations village of Kwalate by a rock avalanche-generated tsunami. *Atmosphere-Ocean*. 45, 123-128; doi:10.3137/ao.450205

Bornhold, B.D., and Thomson, R.E. (2012). Tsunami hazard assessment related to slope failures in coastal waters. In: *Landslides: Types, Mechanisms and Modeling*, ed. John J. Clague and Douglas Stead. Published by Cambridge University Press. Cambridge University Press 2012.

Boyce, R. (2025). Tsunami-causing slide was largest in decade, earthquake center finds, UAF Geophysical Institute, August 12, 2025; https://www.gi.alaska.edu/news/tsunami-causing-slide-was-largest-decade-earthquake-center-finds .

Brideau M.-A., Sturzenegger, M., Stead, D., et al. (2012). Stability analysis of the 2007 Chehalis Lake landslide based on long-range terrestrial photogrammetry and airborne LiDAR data, *Landslides*, 9, 75–91; doi:10.1007/s10346-011-0286-4

Davies, H.L., Davies, J.M., Perembo, R.C.B., and Lus, W.Y. (2003). The Aitape 1998 Tsunami: Reconstructing the Event from Interviews and Field Mapping, *Pure and Applied Geophysics*, 160 (10): 1895–1922.

Dufresne, A., Geertsema, M. Shugar, D.H., et al. (2018). Sedimentology and geomorphology of a large tsunamigenic landslide, Taan Fiord, Alaska, *Sedimentary Geology*, 364, 302-318; doi:10.1016/j.sedgeo.2017.10.004

Evans, S.G. (2001). Landslides. In: *A Synthesis of Geological Hazards in Canada* (ed. Brooks, G. R.), Geological Survey of Canada, Bull. 5.8, 43–79.

Fritz. H.M., Mohammed, F., and Yoo, J. (2009). Lituya Bay landslide impact generated mega-tsunami 50th anniversary, *Pure and Applied Geophysics*, 166, 153-175; doi:10.1007/s00024-008-0435-4.

Geertsema, M., Menounos, B., Bullard, G., Carrivick, J.L., Clague, J.J., et al. (2022). The 28 November 2020 landslide, tsunami, and outburst flood – a hazard cascade associated with

rapid deglaciation at Elliot Creek, British Columbia, Canada, *Geophysical Research Letters*, 49, e2021GL096716; https://doi.org/10.1029/2021GL096716.

Grassi, B., and Karasözen, E. (2025). Major landslide in southeast Alaska fjord, Alaska Earthquake Center, Univ. of Alaska Fairbanks; https://earthquake.alaska.edu/major-landslide-southeast-alaska-fjord

Haeussler, P. J., Gulick, S. P. S. McCall, N., et al. (2018). Submarine deposition of a subaerial Landslide in Taan Fiord, Alaska. *Journal of Geophysical Research, Earth Surface*, 123, 2443-2463; doi:10.1029/2018JF004608

Hamilton, T.S., and Wigen, S.O. (1987). The Foreslope Hills of the Fraser River delta: Implication of tsunamis in Georgia Strait, *Science of Tsunami Hazards*, 5, 15–33.

Higman, B., Shugar, D.H., Stark, C.P., et al. (2018). The 2015 landslide and tsunami in Taan Fiord, Alaska, *Scientific Reports*, 8:12993; doi: 0.1038/s41598-018-30475-w.

Karasözen, E., and West, M.E. (2024). Toward the rapid seismic assessment of landslides in coastal Alaska, *The Seismic Record*, 4(3), 43–51, doi: 10.1785/0320230044.

Kowalik, Z. (1997). Landslide-generated tsunami in Skagway, Alaska, *Science of Tsunami Hazards*, 15 (2), 89-106.

Kulikov, E.A., Rabinovich, A.B., Thomson, R.E., and Bornhold B.D. (1996). The landslide tsunami of November 3, 1994, Skagway Harbor, Alaska, *Journal of Geophysical Research*, 101(C3), 6609-6615.

Kulikov, E.A., Rabinovich, A.B., Fine, I.V., Bornhold, B. D., and Thomson, R. E. (1998). Tsunami generation by landslides at the Pacific coast of North America and the role of tides, *Oceanology*, 38 (3), 323–328.

Lander, J.F. (1996). *Tsunamis Affecting Alaska, 1737–1996*. Boulder, U. S. Dep. Comm., 195 p.

Miller, D.J. (1960). The Alaska earthquake of July 10, 1958: Giant wave in Lituya Bay, *Bulletin of the Seismological Society of America*, 50(2), 253-266; https://doi.org/10.1785/BSSA0500020253

Murty, T.S. (1977). S*eismic Sea Waves– Tsunamis*. Bulletin of the Fisheries Research Board of Canada 198, Ottawa, 337 p.

Murty, T.S. (1979). Submarine slide-generated water waves in Kitimat Inlet, British Columbia, *Journal of Geophysical Research*, 84 (C12), 7777-7779.

Plafker, G., and Greene, H.G. (1998). *Report on the November 3, 1994 Submarine Landslide and Associated Tsunami*, Unpublished Report, July 29, 1998.

Petley, D. (2025). A likely large, tsunamigenic landslide in Tracy Arm inlet, Alaska on 10 August 2025, *EOS*, AGU, 11 August 2025; https://eos.org/thelandslideblog/tracy-arm-1

Prior, D.B., Wiseman, W.J., and Bryant, W.R. (1981). Submarine chutes on the slopes of fjord deltas, *Nature*, 290, 5804, 326–328.

Prior, D.B., Bornhold, B.D., and Johns, M.W. (1984), Depositional characteristics of a submarine debris flow, *Journal of Geology*, 92, 707–727.

Rabinovich, A.B., and Stephenson, F.E. (2004). Longwave measurements for the coast of British Columbia and improvements to the tsunami warning capability, *Natural Hazards*, 32, (3), 313-343.

Rabinovich, A.B., Thomson, R.E., Kulikov, E.A., Bornhold, B.D., and Fine, I.V. (1999). The landslide-generated tsunami of November 3, 1994 in Skagway Harbor, Alaska: A case study, *Geophysical Research Letters,* 26(19), 3009-3012.

Rabinovich, A.B., Thomson, R.E., Bornhold, B.D., Fine, I.V., and Kulikov, E.A., (2003). Numerical modelling of tsunamis generated by hypothetical landslides in the Strait of Georgia, British Columbia, *Pure and Applied Geophysics*, 160(7), 1273-1313.

Rabinovich, A.B., Thomson, R.E., and Fine, I.V. (2013). The 2010 Chilean tsunami off the west coast of Canada and the northwest coast of the United States, *Pure and Applied Geophysics*, 170, 1529-1565; doi: 10.1007/s00024-012-0541-1.

Rabinovich, A.B., Titov, V.V., Moore, C.W., and Eblé, M.C. (2017). The 2004 Sumatra tsunami in the Southeastern Pacific Ocean: New global insight from observations and modeling, *Journal of Geophysical Research: Oceans*, 122 (10), 7992-8019; doi: 10.1002/2017JC013078.

Rabinovich, A.B., Šepić, J., Medvedev, I.P., and Thomson, R.E. (2025). A triple jeopardy flood event: Coincident arrival of the 2022 Tonga tsunami with a storm surge and meteotsunami on the East Coast of the United States. *Bulletin of the American Meteorological Society*, E290-E309. https://doi.org/10.1175/BAMS-D-24-0040.1

Rogers, G.C. (1980). A documentation of soil failure during the British Columbia earthquake of 23 June, 1946, *Canadian Geotechnical Journal*, 17, 122–127.

Shugar, D.H., Barnhart, K.R., Berdah, M., et al. (2026). A 481-meter-high landslide-tsunami in a cruise ship–frequented Alaska fjord. *Science*, doi:10.1126/science.aec3187

Skvortsov, A., and Bornhold, B. (2007). Numerical simulation of the landslide-generated tsunami in Kitimat Arm, British Columbia, Canada, 27 April 1975. *Journal of Geophysical Research*, 112, F02028; https://doi.org/10.1029/2006JF000499

Synolakis, C.E., Bardet, J.-P., Borrero, J.C., Davies, H.L., Okal, E.A., Silver, E. A., Sweet, S., and Tappin, D. R. (2002). The slump origin of the 1998 Papua New Guinea Tsunami. *Proceedings of the Royal Society of London. Series A: Mathematical, Physical and Engineering Sciences*. 458(2020): 763–789. doi:10.1098/rspa.2001.0915.

Terzaghi, K. (1956). Varieties of submarine slope failures. In: *8th Texas Conference on Soil Mechanics and Foundation Engineering* (Houston, Harvard Soil Mech. Comm., 1956), 41 p.

Thomson, R.E., Rabinovich, A.B., Kulikov, E.A., Fine, I.V., and Bornhold, B.D. (2001). On numerical simulation of the landslide-generated tsunami of November 3, 1994 in Skagway Harbor, Alaska, In *Tsunami Research at the End of a Critical Decade,* edited by G. Hebenstreit, Kluwer Acad. Publ., Dordrecht, 243-282.

Thomson R.E., and Emery, W.J. (2024*). Data Analysis Methods in Physical Oceanography*, Fourth Edition. Elsevier Science, Amsterdam, London, New York, 874 p.

Toney, L., Jensen, E., Bilderback, E., et al. (2025). 2025 Tracy Arm landslide-generated tsunami, USGS, Overview; https://www.usgs.gov/programs/landslide-hazards/science/2025-tracy-arm-landslide-generated-tsunami).

Wang, J., Ward, S.N., and Xiao, L. (2015). Numerical simulation of the December 4, 2007 landslide-generated tsunami in Chehalis Lake, Canada, *Geophysical Journal International*, 201, 372–376.

Zaytsev, O., Rabinovich, A.B., and Thomson, R.E. (2024). The 2022 Tonga tsunami on the Pacific and Atlantic coasts of the Americas. *Journal of Geophysical Research: Oceans*, 129, e2024JC020926. https://doi.org/10.1029/2024JC020926